PHYSICAL REVIEW D **83,** 044041 (2011)

Quantum gravity effects in the Kerr spacetime

M. Reuter[1,*] and E. Tuiran[2,†]

[1]*Institute of Physics, University of Mainz, Staudingerweg 7, D-55099 Mainz, Germany*

[2]*Departamento de Física, Universidad del Norte, Km 5 vía a Puerto Colombia, AA-1569 Barranquilla, Colombia*

(Received 13 December 2010; published 24 February 2011)

We analyze the impact of the leading quantum gravity effects on the properties of black holes with nonzero angular momentum by performing a suitable renormalization group improvement of the classical Kerr metric within quantum Einstein gravity. In particular, we explore the structure of the horizons, the ergosphere, and the static limit surfaces as well as the phase space available for the Penrose process. The positivity properties of the effective vacuum energy-momentum tensor are also discussed and the ''dressing'' of the black hole's mass and angular momentum are investigated by computing the corresponding Komar integrals. The pertinent Smarr formula turns out to retain its classical form. As for their thermodynamical properties, a modified first law of black-hole thermodynamics is found to be satisfied by the improved black holes (to second order in the angular momentum); the corresponding Bekenstein-Hawking temperature is not proportional to the surface gravity.

DOI: 10.1103/PhysRevD.83.044041 PACS numbers: 04.70.Dy, 11.10.Gh

I. INTRODUCTION

During the past decade the gravitational average action [1] has been used both as a framework within which the asymptotic safety scenario for a consistent microscopic quantum theory of gravity can be tested [1–22] and as a convenient tool for finding the leading quantum gravity corrections to various classical spacetimes. The latter investigations exploited the effective field theory properties of the average action Γ_k in an essential way. It can be regarded as a one-parameter family of effective field theories, one for each value of the built-in infrared cutoff k [23–26]. In single scale problems involving a typical covariant momentum scale k a tree-level evaluation of Γ_k encapsulates the leading quantum effects at this scale. Thanks to this property the running couplings contained in Γ_k can be used in order to ''renormalization group improve'' the classical field equations or solutions thereof [27–39]. The possibility of interpreting Γ_k as a ''running effective field theory'' distinguishes the effective average action [23] from alternative functionals satisfying exact renormalization group (RG) equations. The functional evolved by Polchinski's equation, for instance, has the interpretation of a bare action. Therefore it cannot be used for ''improvement'' purposes in the same way [25].

Knowing the gravitational average action with some accuracy (i.e. in some truncation) means that we know the scale dependence of a set of generalized gravitational couplings; typically it includes Newton's constant, for instance. These running couplings can be used in order to RG improve classical spacetimes. The basic idea is as follows. One starts by picking a solution of the classical field equation. This solution will in general depend on the classical gravitational couplings. Then one replaces the classical ones by their k-dependent counterparts and tries to express the value of k by means of a ''cutoff identification'' in terms of the relevant geometrical or dynamical scale.

In Refs. [28,29] this approach has been applied to stationary and spherically symmetric, uncharged black holes. The classical starting point was the Schwarzschild metric which involves the classical Newton's constant G_0 in the familiar way. The improvement consisted in replacing the classical G_0 by the running Newton's constant $G(k)$ obtained from the functional RG equation for the effective average action. A subtle point is finding a suitable cutoff identification. It should be chosen in such a way that higher values of k correspond to a ''zooming'' into the details of the black hole. One can try to find a meaningful identification in the form $k = k(\mathcal{P})$ which associates scales to spacetime points $\mathcal{P}$. It is plausible that this map should be such that k is smaller (larger) at larger (smaller) distances from the center of the black hole. In the analogous situation in flat space one would set $k \propto 1/r$, where r is the radial distance; with this identification one can obtain the quantum-corrected Coulomb potential from the k dependence of the fine structure constant, for instance. In gravity the assignment of scales to points should be diffeomorphism invariant; i.e. upon introducing coordinates x^μ the relationship $k = k(\mathcal{P})$ should be represented by a *scalar* function $x^\mu \mapsto k(x^\mu)$. In [28,29] the following class of cutoff identification was considered:

$$k(\mathcal{P}) = \xi/d(\mathcal{P}), \tag{1.1}$$

$$d(\mathcal{P}) = \int_{\mathcal{C}} \sqrt{|ds^2|}. \tag{1.2}$$

Here ξ is a constant of order unity and $d(\mathcal{P})$ is a distance scale typical of the point $\mathcal{P}$. According to (1.2) it is given

*reuter@thep.physik.uni-mainz.de
†etuiran@uninorte.edu.co

 © 2011 American Physical Society

by the length of a certain curve $\mathcal{C}$. This curve is supposed to end at $\mathcal{P}$ and to start at some reference point $\mathcal{P}_0$. The line element ds^2 refers to the classical metric. While diffeomorphism invariant by construction, the above *Ansatz* is still very general and different choices are possible for $\mathcal{C}$. They correspond to different ways of "refocusing" the "microscope" with which spacetime is observed when one goes from one point to another. In Refs. [28,29] a straight radial line from the center to the point $\mathcal{P}$ has been employed, and this choice has been motivated in detail. The only running parameter considered in this analysis was Newton's constant. Its k dependence had been assumed to be given by the formula

$$G(k) = \frac{G_0}{1 + wG_0k^2}. \tag{1.3}$$

Here G_0 is the classical (macroscopic) Newton's constant, and w is a positive constant. This equation is a rather precise approximation to $G(k)$ as obtained from the Einstein-Hilbert truncation [1] for all RG trajectories with a negligible cosmological constant in the classical regime. According to (1.3), the running Newton's constant interpolates between G_0 for $k \to 0$ and the non-Gaussian fixed point behavior $G(k) \propto 1/k^2 \to 0$ for $k \to \infty$. With (1.1) inserted into (1.3) we obtain the position-dependent Newton's constant

$$G(\mathcal{P}) = \frac{G_0 d^2(\mathcal{P})}{d^2(\mathcal{P}) + \bar{w}G_0} \tag{1.4}$$

with $\bar{w} = w\xi^2$.

The RG-improved Schwarzschild metric was obtained by replacing $G_0 \to G(\mathcal{P})$ in the classical metric. It has been analyzed in great detail in [28]. In particular, its horizon structure was investigated. One finds that besides the usual Schwarzschild horizon there exists a new inner horizon which merges with the (standard) outer one at a critical value of the mass. An "extremal" black hole of this kind has vanishing Hawking temperature. In fact the improvement suggests a very attractive scenario for the final state of black-hole evaporation: In the early stages the temperature increases with decreasing mass, as predicted by the conventional semiclassical analysis. However, once the mass approaches the Planck mass, the quantum gravity effects reduce the temperature, and ultimately "switch off" the Hawking radiation. For further details on the RG-improved Schwarzschild black hole we refer to [28] and to [29] where a dynamical picture of the evaporation process by means of a quantum-corrected Vaidya metric has been developed. The generalization to higher dimensions was considered in [38].

The purpose of the present paper is to perform a similar analysis for rotating black holes. We shall construct and analyze an RG-improved version of the Kerr metric. In Boyer-Lindquist coordinates the classical Kerr metric reads [40]

$$ds^2_{\text{class}} = -\left(1 - \frac{2MG_0r}{\rho}\right)dt^2 + \frac{\rho^2}{\Delta}dr^2 + \rho^2 d\theta^2 + \frac{\Sigma \sin^2\theta}{\rho^2}d\varphi^2 - \frac{4MG_0ra\sin^2\theta}{\rho^2}dtd\varphi. \tag{1.5}$$

Here we used the traditional abbreviations

$$\rho^2 \equiv r^2 + a^2\cos^2\theta, \tag{1.6}$$

$$\Delta \equiv r^2 + a^2 - 2MG_0r, \tag{1.7}$$

$$\Sigma \equiv (r^2 + a^2)^2 - a^2\Delta\sin^2\theta. \tag{1.8}$$

Kerr black holes are characterized by two parameters: their mass M and angular momentum $J = aM$ [41–43].

Applying the method outlined above we shall "improve" $ds^2_{\text{class}} \equiv g^{\text{class}}_{\mu\nu}dx^\mu dx^\nu$ by replacing $G_0 \to G(k)$ and using a cutoff identification of the type (1.1). To start with, we are going to analyze various plausible curves $\mathcal{C}$, including a straight radial line again, and discuss their physical properties.

The classical Kerr spacetime has two spherical horizons $H_\pm$ at the radii [44,45]

$$r_\pm = m \pm \sqrt{m^2 - a^2} \tag{1.9}$$

and two static limit surfaces $S_\pm$ at

$$r_{S_\pm}(\theta) = m \pm \sqrt{m^2 - a^2\cos^2\theta}. \tag{1.10}$$

(Here

$$m \equiv MG_0 \tag{1.11}$$

denotes the "geometric mass" which actually has the dimension of a length.) We shall discuss in detail the analogous critical surfaces (horizons and static limit surfaces) of the improved metric. In particular, we demonstrate that, contrary to the Schwarzschild case, the improvement does not lead to the formation of additional horizons.

As compared to the Schwarzschild metric, the Kerr spacetime displays several new features which are interesting from a conceptual point of view. One of them is the existence of an ergosphere and the possibility of extracting energy from the black hole via the Penrose process [45–47]. We shall analyze in detail how the quantum gravity effects influence the structure of the ergosphere and the "phase space" available for the Penrose process.

Another new feature of the Kerr spacetime becomes apparent when one asks whether the improved black holes still satisfy a set of (quantum-corrected) laws of black-hole thermodynamics. In full generality this is an extremely difficult question. Here we can only analyze whether there exists an entropylike state function satisfying a modified version of the first law. In the case of Kerr black holes the space of states, labeled by M and J, is two-dimensional. As a result, it turns out that the mere *existence* of an

entropy is a nontrivial issue. (For the Schwarzschild metric the space is one-dimensional and so the existence of an entropy for the improved black hole is guaranteed.) We shall see that, within the present approach, a state function with the interpretation of an entropy can exist only if the corresponding Hawking temperature is no longer proportional to the surface gravity, as it is semiclassically. At least in the limit of small angular momentum we shall find unambiguously defined relations $T = T(J, M)$ and $S = S(J, M)$ for the temperature and entropy of the improved rotating black holes.

The remaining sections of this paper are organized as follows. In Sec. II we discuss the cutoff identification we are going to employ, and in Sec. III we introduce the RG-improved Kerr metric and analyze some of its general properties; in particular, we derive formulas for the modified static limit and horizon surfaces, we reexpress the metric in a set of appropriately generalized Eddington-Finkelstein coordinates, and we compute the surface gravity of the rotating quantum black holes. Then, in Secs. IV and V we analyze the detailed structure of the critical surfaces and the phase space of the Penrose mechanism (negative energy states), respectively, using both analytical and numerical methods. In Sec. VI we reinterpret the improved vacuum black hole as a classical one in the presence of a certain kind of fictitious matter which mimics the quantum effects, and we investigate the positivity properties of this matter system. In Sec. VII we show how the "bare" mass and angular momentum of these black holes get "dressed" by the quantum effects in accordance with the antiscreening character of quantum Einstein gravity. Finally, in Sec. VIII we take a first step towards an RG-improved black-hole thermodynamics; in particular, we derive a modified first law satisfied by the improved Kerr black holes. Section IX contains a summary of the results.

II. THE CUTOFF IDENTIFICATION

After replacing $G_0 \to G(k)$ we would like to express the scale k as a scalar function on spacetime so that Newton's constant becomes position-dependent:

$$G(r, \theta) \equiv G(k = k(r, \theta)). \tag{2.1}$$

Here we have indicated that for symmetry reasons k and G can depend on the Boyer-Lindquist coordinates r and θ only. The classical spacetime is stationary and invariant under rotations about the z axis; we require that the corresponding Killing vectors [47,48]

$$\mathbf{t} \equiv t^\mu \partial_\mu = \frac{\partial}{\partial t}, \qquad \boldsymbol{\varphi} \equiv \varphi^\mu \partial_\mu = \frac{\partial}{\partial \varphi} \tag{2.2}$$

are Killing vectors of the improved metric, too. If $G(x^\mu)$ is annihilated by $\mathbf{t}$ and $\boldsymbol{\varphi}$, this is indeed the case. In the Boyer-Lindquist (BL) system this means that $G = G(r, \theta)$.

When an explicit form of the "RG trajectory" $G = G(k)$ is needed we shall use the relationship (1.3). However, for our mostly qualitative discussion the precise details of this function are not important. What matters is only that it smoothly interpolates between $G = \text{const}$ in the infrared ($k \to 0$) and $G(k) \propto 1/k^2$ in the ultraviolet ($k \to \infty$). Furthermore, we assume, as in the previous analyses [28,29] that $k(\mathcal{P}) = \xi/d(\mathcal{P})$, which is given by the integral (1.2). In the case at hand it reads

$$d(r, \theta) = \int_{\mathcal{C}(r,\theta)} \sqrt{|ds^2|}, \tag{2.3}$$

where $\mathcal{C}(r, \theta)$ is a path associated to the point $\mathcal{P}$ with BL coordinates (t, r, θ, φ). By stationarity and axial symmetry, $\mathcal{C}$ and d must not depend on t and φ. The line element ds^2 in (2.3) is the one of the classical Kerr metric.

The choice for $\mathcal{C}$ which appears most natural is a radial path from the origin to $\mathcal{P}$. Along this path, $dt = d\theta = d\varphi = 0$ and, by (1.5), $ds^2 = (\rho^2/\Delta)dr^2$. Hence we have in this case

$$d(r, \theta) = \int_0^r d\bar{r} \sqrt{\left| \frac{\bar{r}^2 + a^2 \cos^2\theta}{\bar{r}^2 + a^2 - 2m\bar{r}} \right|}. \tag{2.4}$$

This integral is easy to perform only in the equatorial plane, i.e. for $\theta = \pi/2$. One obtains

$$d(r) \equiv d(r, \pi/2) = \begin{cases} d_1(r) & \text{if } r < r_-, \\ d_2(r) & \text{if } r_- < r < r_+, \\ d_3(r) & \text{if } r_+ < r, \end{cases} \tag{2.5}$$

where $r_\pm$ are the radii of the classical horizons given in (1.9), and [49]

$$d_1(r) = \sqrt{r^2 + a^2 - 2mr} + m \ln\left(\frac{-r + m - \sqrt{r^2 + a^2 - 2mr}}{|a - m|} \right) - a, \tag{2.6}$$

$$d_2(r) = \frac{m}{2} \ln \left| \frac{m + a}{m - a} \right| - a - \sqrt{2mr - r^2 - a^2} + m \arctan\left(\frac{r - m}{\sqrt{2mr - r^2 - a^2}} \right) + \frac{m\pi}{2}, \tag{2.7}$$

$$d_3(r) = \sqrt{r^2 + a^2 - 2mr} + m \ln(r - m + \sqrt{r^2 + a^2 - 2mr}) + \pi m - a - m \ln|m - a|. \tag{2.8}$$

The function $d(r)$ for the equatorial plane is displayed in Fig. 1 for a black hole with a mass of $10 m_{\text{Pl}}$ and for various values of the angular momentum parameter a. [In this and the following figures all dimensionful quantities are expressed in units of the Planckian quantities formed with the infrared value of Newton's constant, $\ell_{\text{Pl}} = m_{\text{Pl}}^{-1} = \sqrt{G_0}$. Since a, m, r, and $d(r)$ have the dimension of a length they are measured in units of ℓ_{Pl}. As $m \equiv G_0 M$ by definition,

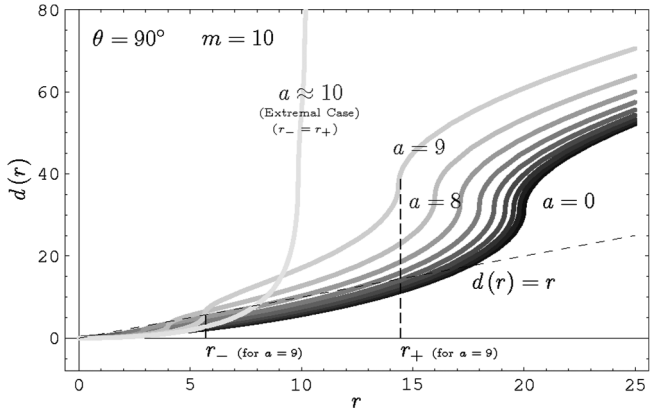

FIG. 1. The radial distance $d(r)$ in the equatorial plane for $m = 10$ and various values of a. All quantities are expressed in Planck units. The gray scale runs from black to gray for increasing a.

the geometric mass m equals the actual mass M when Planck units are used.]

The main features of the $d(r)$ curves are as follows. For $a < m$ not too close to the extreme case $a = m$, the curves run essentially parallel to the dashed line in Fig. 1, representing the function $d(r) = r$. At their respective values of r_- and r_+, all curves have a vertical tangent. Near the classical horizon radii $r_\pm$ the functions $d(r)$ shift away from the $d(r) = r$ line by a kind of smoothed-out step function. At a sufficient distance from $r_\pm$ they run parallel to $d(r) = r$. In particular, for $r \gg r_+$ the exact $d(r)$ is approximately of the form $d(r) \approx r + \Delta d$, where Δd is a constant independent of r. Obviously, for r large enough so that $\Delta d/r \ll 1$, we can approximate the $d(r)$ curves simply by $d(r) = r$. For smaller r there is the steplike behavior near r_- and r_+, but in most of our qualitative investigations it will not play a role. The deviations from $d(r) = r$ become significant when a approaches m which corresponds to the situation of an extremal classical black hole.

For $\theta \neq \pi/2$ it is easy to evaluate the integral (2.4) numerically. It turns out that $d(r, \theta)$ has a similar r dependence for all values of θ. For $\theta < \pi/2$ the shift Δd is somewhat larger than at the equator, but nevertheless all curves are essentially parallel to $d(r) = r$ again.

A more precise asymptotic analysis of the integral (2.4) reveals that $d(r, \theta)$ has the following structure for $r \to \infty$:

$$d(r, \theta) = r + m \ln(r) + F(\theta) + O\left(\frac{1}{r}\right). \tag{2.9}$$

There are three types of terms which do not vanish for $r \to \infty$: a linearly increasing one, a logarithmically increasing one, and one which is r-independent. Among the three, only the r-independent one depends on the angle θ. Since $F(\theta)$ is subdominant we see that, to logarithmic accuracy, $d(r, \theta)$ is actually independent of θ at large r.

An alternative definition of the distance scale $d(r, \theta)$ could be as follows [45]. Let $\mathcal{C}(r, \theta)$ be a circular path of coordinate radius r, contained in the $\theta =$ const plane and centered about the origin. In this case we define $d(r, \theta)$ to be the *reduced circumference* of this path, i.e. its proper length divided by 2π. In flat space the reduced circumference would equal r; in the Kerr background there are corrections. A detailed numerical analysis [49] shows that, for r not too small and a not too close to m, the resulting distance functions $d(r, \theta)$ have similar qualitative properties as those from the radial path.

For concreteness we shall use the distance function obtained from the radial path whenever a concrete expression is needed. Since our analysis is mostly at a qualitative or "semiquantitative" level we shall be concerned with leading order effects only. For this reason we shall neglect the subdominant θ dependence of $d(r, \theta)$ and assume that $d \equiv d(r)$ and, as a result G, depends on r only:

$$G(r) \equiv G(k = \xi/d(r)). \tag{2.10}$$

The implications of the θ dependence are presumably too weak to be accessible by our present method.

III. GENERAL PROPERTIES OF THE IMPROVED KERR METRIC

From now on we assume that we are given a r-dependent Newton's constant, $G = G(r)$. It may arise by inserting the cutoff identification $k \propto 1/d(r)$ into a solution of the RG equation such as (1.3), but for most parts of our discussion the actual origin of the r dependence is irrelevant.

A. The quantum-corrected metric

Substituting $G_0 \to G(r)$ in (1.5) we arrive at the improved Kerr metric in BL coordinates:

$$ds_I^2 = g_{tt}dt^2 + 2g_{t\varphi}dtd\varphi + g_{rr}dr^2 + g_{\theta\theta}d\theta^2 + g_{\varphi\varphi}d\varphi^2 \tag{3.1}$$

with the components

$$g_{tt} = -\left(1 - \frac{2MG(r)r}{\rho^2}\right), \quad g_{rr} = \frac{\rho^2}{\Delta_I(r)}, \quad g_{\varphi\varphi} = \frac{\Sigma_I(r, \theta)\sin^2\theta}{\rho^2}, \tag{3.2}$$

$$g_{\theta\theta} = \rho^2, \qquad g_{t\varphi} = -\frac{2MG(r)ra\sin^2\theta}{\rho^2}. \tag{3.3}$$

Here $\rho^2 \equiv r^2 + a^2\cos^2\theta$ is unchanged, but Δ and Σ contain $G(r)$ now:

$$\Delta_I(r) \equiv r^2 + a^2 - 2MG(r)r, \tag{3.4}$$

$$\Sigma_I(r, \theta) \equiv (r^2 + a^2)^2 - a^2\Delta_I(r)\sin^2\theta. \tag{3.5}$$

For later use we also note the components of the inverse metric tensor:

$$g^{tt} = -\frac{\Sigma_I}{\rho^2\Delta_I}, \qquad g^{rr} = \frac{\Delta_I}{\rho^2}, \qquad g^{\varphi\varphi} = \frac{\Delta_I - a^2\sin^2\theta}{\rho^2\Delta_I\sin^2\theta}, \tag{3.6}$$

$$g^{\theta\theta} = \frac{1}{\rho^2}, \qquad g^{t\varphi} = -\frac{2MG(r)ra}{\rho^2\Delta_I}. \tag{3.7}$$

In the rest of this section we shall describe various general properties of the metric (3.1) and (3.2). The discussion parallels the classical case to some extent [48], but the results collected here will be needed for an analysis of the quantum effects.

B. Killing vectors and conserved quantities

We mentioned already that the improved metric has the Killing vector $\boldsymbol{t}$ and $\boldsymbol{\varphi}$ of Eq. (2.2). If we employ BL coordinates, its components are obviously

$$t^\mu = \delta^\mu_t, \qquad \varphi^\mu = \delta^\mu_\varphi \quad \text{(BL)}. \tag{3.8}$$

Considering a point particle of mass m which moves along the trajectory $x^\mu(\tau)$ with four-velocity $u^\mu \equiv dx^\mu/d\tau$ and momentum $p^\mu = mu^\mu$ these Killing vectors imply a conserved energy and angular momentum about the symmetry axis [47]:

$$\begin{aligned} E &= -t_\mu p^\mu \equiv -mt_\mu u^\mu, \\ L &= -\varphi_\mu p^\mu \equiv -m\varphi_\mu u^\mu. \end{aligned} \tag{3.9}$$

C. Zero angular momentum, static, and stationary observers

We consider three classes of special "observers" (actually point particles) following a world line $x^\mu(\tau)$, parametrized by the proper time τ, with the velocity $u^\mu = dx^\mu(\tau)/d\tau \equiv \dot{x}^\mu$, $u^\mu u_\mu = -1$. (A dot will always denote the derivative with respect to τ.)

1. Zero angular momentum observers

By definition zero angular momentum observers (or "ZAMOs") are particles with vanishing L: $0 = L = mg_{\mu\nu}\dot{x}^\mu\varphi^\nu$. When evaluated in BL coordinates, this condition reads $g_{t\varphi}\dot{t} + g_{\varphi\varphi}\dot{\varphi} = 0$. Parametrizing the ZAMO's world line by the coordinate time t rather than the proper time τ, the condition assumes the form $g_{t\varphi} + g_{\varphi\varphi}(d\varphi/dt) = 0$. Therefore, introducing the angular velocity with respect to the coordinate time,

$$\Omega \equiv \frac{d\varphi}{dt}, \tag{3.10}$$

as well as the convenient abbreviation

$$\omega \equiv \omega(r,\theta) \equiv -\frac{g_{t\varphi}}{g_{\varphi\varphi}} = -\frac{2G(r)Mar}{\Sigma_I}, \tag{3.11}$$

we conclude that even though they have no angular momentum, the ZAMOs rotate around the z axis with the angular velocity

$$\Omega^{\text{ZAMO}} = \omega. \tag{3.12}$$

The quantity $\omega \geq 0$ is the coordinate angular velocity with which inertial frames are dragged along [44,45,47,50]. It is affected by the r dependence of G on which it depends both explicitly and via Σ_I.

2. Static observers

By definition, the four-velocity of static observers is proportional to the Killing vector $\boldsymbol{t}$, i.e. $u^\mu = \gamma t^\mu$, where γ is chosen as $\gamma = [-g_{\mu\nu}t^\mu t^\nu]^{-(1/2)}$ in order to achieve $u_\mu u^\mu = -1$. The motion of static observers is not geodesic. To follow their world line they will need a rocket engine, say. Static observers exist only in those portions of the improved Kerr spacetime in which $\boldsymbol{t}$ is timelike. The *"static limit"* is reached when $\boldsymbol{t}$ becomes null, i.e. when $\gamma^{-2} = -g_{\mu\nu}t^\mu t^\nu = 0$. In BL coordinates this is the case where $g_{tt} = 0$, or explicitly,

$$r^2 - 2G(r)Mr + a^2\cos^2\theta = 0. \tag{3.13}$$

In the classical case the solution to this condition are two static limit surfaces $S_\pm$ which can be parametrized as $r = r_{S_\pm}(\theta)$ with $r_{S_\pm}(\theta)$ given in (1.10). For the improved metric the situation will be more complicated; depending on the values of M and a there can be two, one, or no static limit surface S at all. Also in the improved case, since $g_{tt} = 0$ on S, static limit surfaces are surfaces of infinite redshift.

3. Stationary observers

A way of defining event horizons, different from their characterization as one-way surfaces, is related to stationary observers. By definition a stationary observer moves with a constant angular velocity $\Omega = d\varphi/dt$ in the φ direction. Its four-velocity is proportional to the Killing vector $\boldsymbol{\xi} = \boldsymbol{t} + \Omega\boldsymbol{\varphi}$, i.e. $u^\mu = \gamma(t^\mu + \Omega\varphi^\mu) = \gamma\xi^\mu$. This class of observers is stationary in the sense that they perceive no time variation of the gravitational field. They exist only if Ω and the *constant* parameters of their orbit, r and φ, are such that $\gamma^{-2} = -g_{\mu\nu}\xi^\mu\xi^\nu > 0$. In BL coordinates this condition boils down to

$$q(\Omega) \equiv \Omega^2 - 2\omega\Omega + g_{tt}/g_{\varphi\varphi} < 0. \tag{3.14}$$

If

$$\Omega_\pm = \omega \pm \sqrt{\omega^2 - g_{tt}/g_{\varphi\varphi}} \tag{3.15}$$

is real, the function q has two zeros on the real axis, and (3.14) is satisfied if $\Omega_- < \Omega < \Omega_+$. Depending on whether g_{tt}, evaluated at the (r,θ) values of the orbit, is negative, zero, or positive qualitatively different situations

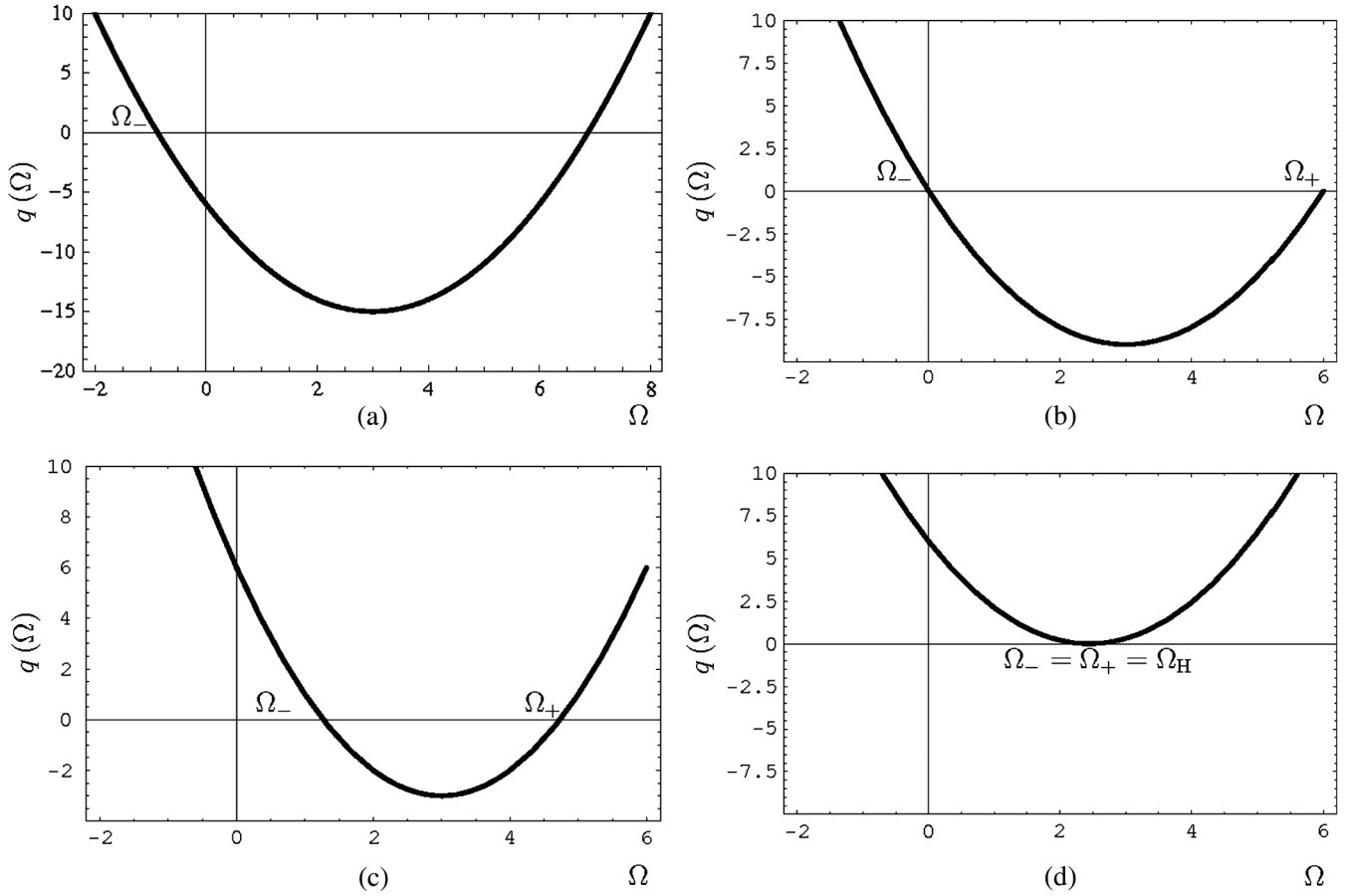

FIG. 2. The function $q(\Omega)$ in the 4 cases discussed in the text.

can occur. The corresponding graph of $q(\Omega)$ is sketched in Fig. 2. Let us discuss the 4 cases depicted there in turn.

(1) The case $g_{tt} < 0$.—In this case $\sqrt{\omega^2 - g_{tt}/g_{\varphi\varphi}} = \sqrt{\omega^2 + |g_{tt}/g_{\varphi\varphi}|} > \omega$ since $g_{\varphi\varphi} > 0$ for all $r > 0$ and $\theta \neq 0, \pi$. Therefore since $\omega \geq 0$, it follows that $\Omega_- < 0$ and $\Omega_+ < 0$. Stationary observers exist for $\Omega \in (\Omega_-, \Omega_+)$. Those with $\Omega \in (\Omega_-, 0)$ are rotating in the opposite direction as the black hole, and those with $\Omega \in (0, \Omega_+)$ rotate in the same direction. Static observers correspond to the special case $\Omega = 0$. The case $g_{tt} < 0$ is depicted in Fig. 2(a).

(2) The case $g_{tt} = 0$.—In this case $\Omega_- = 0$ and $\Omega_+ = 2\omega > 0$. There are no counterrotating ($\Omega < 0$) observers any more; stationary observers are necessarily corotating with the black hole. Counterrotating light rays are bound to stay static with $\Omega \equiv \Omega_- = 0$ [see Fig. 2(b)].

(3) The case $g_{tt} > 0$.—Here $\sqrt{\omega^2 - g_{tt}/g_{\varphi\varphi}} < \omega$ and therefore $\Omega_- > 0$ and $\Omega_+ > 0$. All stationary observers are corotating with strictly positive angular velocity $\Omega \in (\Omega_-, \Omega_+)$. There are no static observers.

(4) The case $\Delta_I = 0$.—Using the explicit form of the metric components, the frequencies $\Omega_\pm$ can always be written as [48,49]

$$\Omega_\pm = \omega \pm \frac{\Delta_I^{1/2}\rho^2}{\Sigma_I \sin\theta}. \tag{3.16}$$

This implies that when $\Delta_I = 0$ the two frequencies become equal: $\Omega_+|_{\Delta_I=0} = \Omega_-|_{\Delta_I=0} = \omega|_{\Delta_I=0} = 0$. At a radius r such that $\Delta_I(r) = 0$ stationary observers are forced to rotate precisely with the angular velocity ω about the black hole. The condition $\Delta_I = 0$ is equivalent to $g^{rr} = 0$. Therefore using the same argument as classically [48], one sees that it defines an event horizon of the improved Kerr spacetime.

We shall find that under the condition $M \gg m_{\rm Pl}$ the improved spacetime has two spherical horizons $H_\pm$ and two limit surfaces $S_\pm$ exactly like the classical one. The radii of the static limit surfaces, $r^I_{S_\pm}(\theta) \equiv r^I_S(\theta)$, satisfy

$$g^{rr} = 0 \Leftrightarrow (r^I_S)^2 - 2G(r^I_S)Mr^I_S + a^2\cos^2\theta = 0, \tag{3.17}$$

while the radii of the horizons, $r^I_\pm \equiv r^I_H$, are such that

$$\Delta_I(r^I_H) = 0 \Leftrightarrow (r^I_H)^2 - 2G(r^I_H)Mr^I_H + a^2 = 0. \tag{3.18}$$

The 4 surfaces can be ordered by increasing radius:

$$r^I_{S_-}(\theta) \le r^I_- \le r^I_+ \le r^I_{S_+}(\theta). \tag{3.19}$$

Here as always, the label "I" stands for improved.

If one decreases r at fixed θ, the 4 cases occur in the above order: For $r > r^I_{S_+}(\theta)$, outside the static limit, case (1) is realized. At $r = r^I_{S_+}(\theta)$ we have $g_{tt} = 0$ and case (2) applies. Between S_+ and H_+, in the ergosphere, we have (3), and all stationary observers with $r \in (r^I_+, r^I_{S_+}(\theta))$ necessarily rotate in the direction of the black hole. When we approach $r = r^I_+$ from above the only allowed angular velocity is

$$\Omega_+ = \Omega_- = \omega(r^I_+, \theta) \equiv \Omega_H. \tag{3.20}$$

For $r < r^I_+$, there exist no stationary observers any longer: Once it has crossed the horizon H_+, a particle necessarily falls into the black hole. We shall refer to Ω_H as "the angular velocity of the black hole." Noting that $\Omega_H = 2G(r^I_+)Mar^I_+/\Sigma_I(r^I_+, \theta)$ with $\Sigma_I(r^I_+, \theta) = [(r^I_+)^2 + a^2]^2 - a^2\Delta_I(r^I_+)\sin^2\theta = [(r^I_+)^2 + a^2]^2$ we observe that Ω_H is actually independent of the angle θ and depends only on the parameters M and a:

$$\Omega_H(M, a) = \frac{a}{r^I_+(M, a)^2 + a^2}. \tag{3.21}$$

This formula looks like its classical counterpart [48]; however, the improvement changes the M and a dependence of r^I_+.

D. Generalized Eddington-Finkelstein coordinates

The systems of Boyer-Lindquist coordinates (t, r, θ, φ) breaks down when $\Delta_I = 0$, i.e. on a possible horizon. In order to reexpress the improved Kerr metric in a system of coordinates which remains regular there, we define a generalization of the familiar advanced time (or ingoing) Eddington-Finkelstein (EF) coordinates [47,48]:

$$v = t + r^*(r), \qquad r = r, \qquad \theta = \theta, \qquad \psi = \varphi + r^\#(r). \tag{3.22}$$

Here the functions r^* and $r^\#$ are given by

$$r^*(r) \equiv \int^r dr' \frac{r'^2 + a^2}{\Delta(r')} = \int^r dr' \frac{r'^2 + a^2}{r'^2 - 2Mr'G(r') + a^2},$$
$$r^\#(r) \equiv \int^r dr' \frac{a}{\Delta(r')} = \int^r dr' \frac{a}{r'^2 - 2Mr'G(r') + a^2}. \tag{3.23}$$

For a constant $G(r)$ these integrals can be performed in closed form. For the improved metric this is not possible in general. Luckily the explicit forms of r^* and $r^\#$ are not needed in order to express the metric in terms of the new coordinates $x^\mu = (v, r, \theta, \psi)$. It is enough to use that by (3.23) $dt = dv - (r'^2 + a^2)\Delta_I^{-1}dr$ and $d\varphi = d\psi - a\Delta_I^{-1}dr$. Inserting these differentials into (3.1) we obtain the following line element for the improved Kerr metric in ingoing EF coordinates:

$$ds^2_I = -\left(1 - \frac{2G(r)Mr}{\rho^2}\right)dv^2 + 2drdv - 2a\sin^2\theta d\psi dr - \frac{4G(r)Mar\sin^2\theta}{\rho^2}d\psi dv + \frac{\Sigma_I\sin^2\theta}{\rho^2}d\psi^2 + \rho^2 d\theta^2. \tag{3.24}$$

We shall also need the Killing vector $\boldsymbol{\xi} = \boldsymbol{t} + \Omega_H\boldsymbol{\varphi}$ in EF coordinates. It is trivial to see that $\boldsymbol{\xi} = \frac{\partial}{\partial v} + \Omega_H\frac{\partial}{\partial\varphi}$, i.e.

$$\xi^v = 1, \qquad \xi^r = 0, \qquad \xi^\theta = 0, \qquad \xi^\psi = \Omega_H. \tag{3.25}$$

Using the metric (3.24) one obtains the following expression for the square $\boldsymbol{\xi}^2 = g_{\mu\nu}\xi^\mu\xi^\nu$:

$$\boldsymbol{\xi}^2 = \frac{\Sigma_I\sin^2\theta}{\rho^2}(\omega - \Omega_H)^2 - \frac{\rho^2\Delta_I}{\Sigma_I}. \tag{3.26}$$

This scalar function is well defined both away from and directly on H_+. In fact, it vanishes on the horizon, $\boldsymbol{\xi}^2|_{H_+} = 0$, since $\Delta_I = 0$ and $\omega = \Omega_H$ there. This is exactly as it should be: In Sec. III C 3 we saw that $\gamma^{-2} = -\boldsymbol{\xi}^2 \propto q(\Omega_H)$, and since $q(\Omega_H) = 0$, the Killing vector becomes null on the horizon.

E. Quantum corrections to the surface gravity

As the improved Kerr metric admits a Killing vector which is null at the event horizon and tangent to the horizon's null generators we may define the surface gravity κ in the usual way [48]:

$$-D_\mu\boldsymbol{\xi}^2(r^I_+) = 2\kappa\xi_\mu(r^I_+). \tag{3.27}$$

To determine κ we shall evaluate (3.27) in the generalized EF coordinates introduced in the previous subsection. On the right-hand side (RHS) of (3.27) we insert $\xi_\mu = g_{\mu v} + \Omega_H g_{\mu\psi}$, which, in EF coordinates, evaluates to

$$\xi_\mu(r^I_+) = [1 - a\Omega_H\sin^2\theta]\partial_\mu r = \frac{(r^I_+)^2 + a^2\cos^2\theta}{(r^I_+)^2 + a^2}\partial_\mu r. \tag{3.28}$$

In deriving (3.28) we made repeated use of the horizon condition (3.18). On the left-hand side (LHS) of (3.27) we need the derivative $D_\mu\boldsymbol{\xi}^2 \equiv \partial_\mu\boldsymbol{\xi}^2$ of the function $\boldsymbol{\xi}^2$ given in Eq. (3.26), evaluated at $r = r^I_+$. Since $\Delta_I = 0$ and $(\omega - \Omega_H) = 0$ there, one easily finds

$$-D_\mu\boldsymbol{\xi}^2(r^I_+) = \frac{(r^I_+)^2 + a^2\cos^2\theta}{[(r^I_+)^2 + a^2]^2}\Delta'_I(r^I_+)\partial_\mu r. \tag{3.29}$$

As a result, the surface gravity is given by

$$\kappa = \frac{1}{2}\frac{\Delta'_I(r^I_+)}{(r^I_+)^2 + a^2}, \tag{3.30}$$

where the prime, as always, denotes a derivative with respect to the argument. More explicitly,

$$\kappa = \frac{r_+^I - G(r_+^I)M - r_+^I G'(r_+^I)M}{(r_+^I)^2 + a^2}. \tag{3.31}$$

Several comments are in order here.

(a) For $G(r) = \text{const}$, Eq. (3.31) coincides with the classical result. The quantum corrections modify κ both explicitly, by the $G'(r_+^I)$ term, and implicitly, via the shift in the radius r_+^I.

(b) The surface gravity of the improved metric has turned out independent of θ. It is constant on H_+ therefore. This is nontrivial since the symmetry assumptions imply only φ but no θ independence. Classically, $\kappa = \text{const}$ constitutes the zeroth law of black-hole thermodynamics where κ is related to the Bekenstein-Hawking temperature via $T = \kappa/2\pi$ [51,52]. In Sec. VIII we shall address the question of whether a similar interpretation can hold in the improved case.

(c) As in the classical case, κ vanishes for extremal black holes. Their $\Delta(r)$ has a double zero at the horizon, implying $\Delta = \Delta' = 0$ there.

(d) Sometimes it is convenient to rewrite κ in a way which removes any explicit a dependence. Again exploiting $\Delta_I(r_+^I) = 0$ yields

$$\kappa = \frac{1}{2G(r_+^I)M} - \frac{1}{2r_+^I} - \frac{G'(r_+^I)}{2G(r_+^I)}. \tag{3.32}$$

Of course, κ continues to be implicitly a-dependent via r_+^I.

(e) For $a = 0$ the horizon condition is $r_+^I = 2G(r_+^I)M$. Using this relation in (3.32) we obtain the surface gravity for the improved Schwarzschild metric:

$$\kappa = \frac{1}{4G(r_+^I)M} - \frac{G'(r_+^I)}{2G(r_+^I)}. \tag{3.33}$$

Assuming the validity of $T = \kappa/2\pi$ for the Schwarzschild black hole, Eq. (3.33) implies exactly the Hawking temperature which had been found in Ref. [28] using a rather different argument.

IV. HORIZONS AND STATIC LIMIT SURFACES

A. Critical surfaces

In this section we determine the horizons and the static limit surfaces of the improved Kerr metric. We shall collectively refer to them as "critical surfaces." In Sec. III we saw that the radii $r_S^I(\theta)$ and r_H^I of a static limit surface S and a horizon H are given by Eqs. (3.17) and (3.18), respectively. By defining

$$b \equiv \begin{cases} a\cos\theta & \text{for } S \\ a & \text{for } H \end{cases} \tag{4.1}$$

those two equations can be combined into one, namely,

$$r^2 - 2G(r)Mr + b^2 = 0. \tag{4.2}$$

With a $G(r)$ of the form (1.4), i.e.

$$G(r) = \frac{G_0 d^2(r)}{d^2(r) + \bar{w}G_0}, \tag{4.3}$$

this condition becomes

$$\tilde{d}^{\,2}(\tilde{r})(\tilde{r}^2 + \tilde{b}^2 - 2\tilde{m}\,\tilde{r}) + \bar{w}(\tilde{r}^2 + \tilde{b}^2) = 0. \tag{4.4}$$

Here and in the following the tilde means that the corresponding quantity is expressed in terms of the Planck units related to G_0. In particular, $\tilde{r} = r/\ell_{\rm Pl}$, $\tilde{m} = m/\ell_{\rm Pl}$, $\tilde{M} = M/m_{\rm Pl}$, $\tilde{a} = a/\ell_{\rm Pl}$, $\tilde{b} = b/\ell_{\rm Pl}$, and $\tilde{d} = d/\ell_{\rm Pl}$, where $G_0 \equiv m_{\rm Pl}^{-2} \equiv \ell_{\rm Pl}^2$. Thus we are led to investigate possible zeros of the family of functions

$$Q_{\tilde{b}}^{\bar{w}}(\tilde{r}) \equiv \tilde{d}^2(\tilde{r})(\tilde{r}^2 + \tilde{b}^2 - 2\tilde{m}\,\tilde{r}) + \bar{w}(\tilde{r}^2 + \tilde{b}^2). \tag{4.5}$$

Depending on our choice for the parameters $\tilde{b}$ and $\bar{w}$ Eq. (4.5) describes the critical surfaces of the following metrics:

(1) classical Schwarzschild metric: $\bar{w} = 0$, $\tilde{b} = 0$;
(2) classical Kerr metric: $\bar{w} = 0$, $\tilde{b} \neq 0$;
(3) improved Schwarzschild metric: $\bar{w} \neq 0$, $\tilde{b} = 0$;
(4) improved Kerr metric: $\bar{w} \neq 0$, $\tilde{b} \neq 0$.

We shall analyze (4.5) for the distance function $d(r)$ obtained from the straight radial path $\mathcal{C}$ discussed in Sec. II. We proceed in two steps: We first employ the simple approximation $d(r) = r$ for an analytic discussion of the problem, and then in a second step, we use numerical methods to show that, qualitatively, the results obtained analytically are indeed representative and provide us with a correct picture of the new features which are due to the nonzero angular momentum of the black hole.

B. The approximation $d(r) = r$

For $d(r) = r$ the function $Q_{\tilde{b}}^{\bar{w}}$ becomes a quartic polynomial:

$$Q_{\tilde{b}}^{\bar{w}}(\tilde{r}) \equiv \tilde{r}^4 - 2\tilde{m}\tilde{r}^3 + (\tilde{b}^2 + \bar{w})\tilde{r}^2 + \bar{w}\tilde{b}^2. \tag{4.6}$$

Before turning to the general case of the improved Kerr metric it is instructive to see how the critical surfaces arise in the special cases (1), (2), and (3):

(1) *The classical Schwarzschild metric.*—In this case the polynomial simplifies to

$$Q_0^0(\tilde{r}) \equiv \tilde{r}^3(\tilde{r} - 2\tilde{m}). \tag{4.7}$$

It has a triple zero at $\tilde{r} = 0$ and a simple zero at $\tilde{r} = 2\tilde{m}$, or $r = 2G_0M$.

(2) *The classical Kerr metric.*—Here the function (4.6) becomes

$$Q_{\tilde{b}}^0(\tilde{r}) \equiv \tilde{r}^2(\tilde{r}^2 - 2\tilde{m}\,\tilde{r} + \tilde{b}^2). \tag{4.8}$$

It has a double zero at $\tilde{r} = 0$ and two simple zeros at

$$\tilde{r}_{\,\pm} = \tilde{m} \pm \sqrt{\tilde{m}^2 - \tilde{b}^2} \tag{4.9}$$

if $\tilde{m} \neq \tilde{b}$ or one double zero at $\tilde{r} = \tilde{m}$ if $\tilde{m} = \tilde{b}$. These zeros give rise to the familiar static limit surfaces $S_\pm$ and horizons $H_\pm$ at

$$r_{S_\pm}(\theta) = G_0M \pm \sqrt{(G_0M)^2 - a^2\cos^2\theta}, \quad (4.10)$$

$$r_\pm \equiv r_{H_\pm} = G_0M \pm \sqrt{(G_0M)^2 - a^2}. \quad (4.11)$$

In the case $\tilde{m} = \tilde{a}$ the two horizons H_+ and H_- merge to a simple one with the "critical" radius $\tilde{r} = \tilde{m}$. We then have an extremal black hole with $a = G_0M$, or $J \equiv aM = G_0M^2$, and $r_{\rm crit} = G_0M_{\rm crit} = a$ [53].

(3) *The improved Schwarzschild metric*.—In this case (4.6) reads

$$Q_0^{\bar{w}}(\tilde{r}) = \tilde{r}^2(\tilde{r}^2 - 2\tilde{m}\,\tilde{r} + \bar{w}). \quad (4.12)$$

This function has a double zero at $\tilde{r} = 0$ and two simple zeros at

$$\tilde{r}^{\,I}_\pm = \tilde{m} \pm \sqrt{\tilde{m}^2 - \bar{w}} \quad (4.13)$$

if $\tilde{m}^2 \neq \bar{w}$ or one double zero at $\tilde{r}^I = \tilde{m}$ if $\tilde{m}^2 = \bar{w}$. As a result, the quantum-corrected Schwarzschild spacetime has two spherical horizons $H_\pm$ at

$$r^I_\pm = G_0M \pm \sqrt{(G_0M)^2 - \bar{w}G_0}. \quad (4.14)$$

If $\tilde{m}^2 = \bar{w}$, the two horizons coalesce to a single one at the critical radius $r_{\rm cr} = \sqrt{\bar{w}}\ell{\rm Pl} = G_0M_{\rm cr}$. This new type of an extremal black hole is realized when the mass equals the critical mass $M_{\rm cr} = \sqrt{\bar{w}}m_{\rm Pl}$. Since $\bar{w} = O(1)$ extremal black holes have a mass of the order of $m_{\rm Pl}$. For $M < M_{\rm cr}$ the improved Schwarzschild metric has no horizon at all. The improved Schwarzschild metric has been discussed in detail in Ref. [28] to which the reader is referred for further details.

As for the existence of horizons it is also interesting to note that there is a close analogy between the *classical* Kerr metric and the *improved* Schwarzschild metric. The above formulas are identical if one identifies $\tilde{a}^2$ with $\bar{w}$ or, for the dimensionful quantities a^2, with $\bar{w}G_0$.

Note that in going from case (1) to either case (2) or case (3) the triple zero at $\tilde{r} = 0$ turns into a double zero at $\tilde{r} = 0$, plus a simple zero at $\tilde{r} > 0$.

(4) *The improved Kerr metric*.—Finally we discuss the zeros of $Q^{\bar{w}}_{\tilde{b}}$ with both $\bar{w}$ and $\tilde{b}$ nonzero. In principle their dependence on $\tilde{m}$, $\tilde{b}$, and $\bar{w}$ could be written down in closed form but the formulas are not very instructive. The following indirect reasoning shows the essential points more clearly.

The first and second derivatives of $Q^{\bar{w}}_{\tilde{b}}$ are

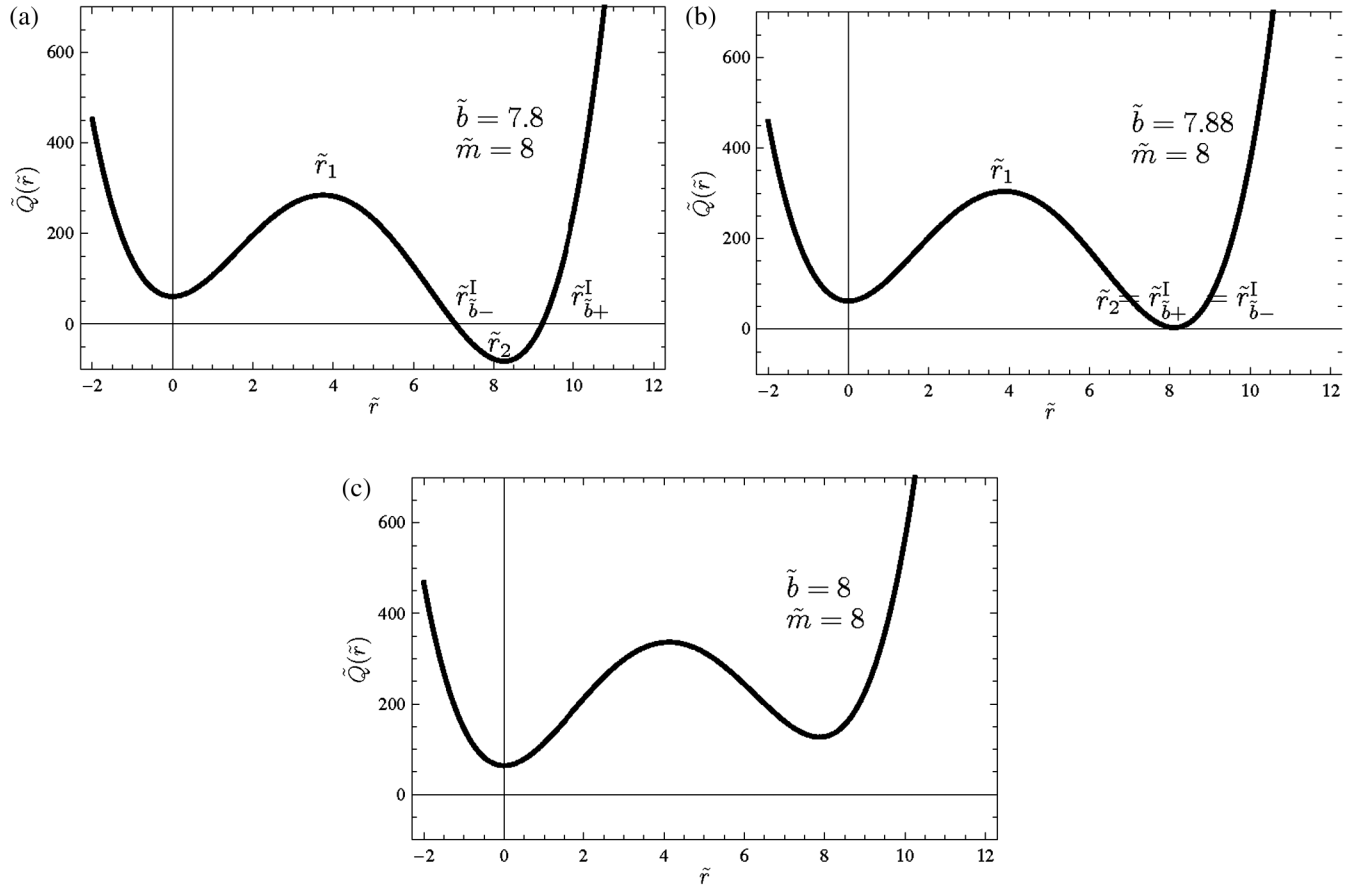

FIG. 3. The figures show examples of the 3 possible configurations the function $Q^{\bar{w}}_{\tilde{b}}$ of Eq. (4.6) can assume, with two, one, and no zero on the positive real axis.

$$\frac{d}{d\tilde{r}} Q^{\bar{w}}_{\tilde{b}}(\tilde{r}) = 2\tilde{r}[2\tilde{r}^2 - 3\tilde{m}\,\tilde{r} + (\tilde{b}^2 + \bar{w})], \quad (4.15)$$

$$\frac{d^2}{d\tilde{r}^2} Q^{\bar{w}}_{\tilde{b}}(\tilde{r}) = 12\tilde{r}^2 - 12\tilde{m}\,\tilde{r} + 2(\tilde{b}^2 + \bar{w}). \quad (4.16)$$

The derivative (4.15) vanishes at the $\tilde{r}$ values $\tilde{r}_0$, $\tilde{r}_1$, and $\tilde{r}_2$ given by

$$\begin{aligned} \tilde{r}_0 &= 0, \\ \tilde{r}_1 &= \frac{3}{4}\tilde{m}\left[1 - \sqrt{1 - \frac{8}{9}\frac{\tilde{b}^2 + \bar{w}}{\tilde{m}^2}}\right], \\ \tilde{r}_2 &= \frac{3}{4}\tilde{m}\left[1 + \sqrt{1 - \frac{8}{9}\frac{\tilde{b}^2 + \bar{w}}{\tilde{m}^2}}\right]. \end{aligned} \quad (4.17)$$

Provided

$$\tfrac{8}{9}(\tilde{b}^2 + \bar{w}) \leq \tilde{m}^2, \quad (4.18)$$

the square roots in (4.17) are real so that $\tilde{r}_1$ and $\tilde{r}_2$ are real and positive. As a result, $Q^{\bar{w}}_{\tilde{b}}$ has 3 different extrema for $\tilde{r} \geq 0$, except when the equality sign holds in (4.18). Then two extrema merge to an inflection point. Inserting (4.17) into (4.16) one finds that the second derivative is negative at $\tilde{r}_1$ and positive at $\tilde{r}_0$ and $\tilde{r}_2$. Therefore in the nondegenerate case, $\tilde{r}_0$ and $\tilde{r}_2$ are minima, and $\tilde{r}_1$ is a maximum of $Q^{\bar{w}}_{\tilde{b}}$. If $\frac{8}{9}(\tilde{b}^2 + \bar{w}) = \tilde{m}^2$, there is a minimum at $\tilde{r}_0 = 0$ and an inflection point at $\tilde{r}_1 = \tilde{r}_2 = 3\tilde{m}/4$, and if $\frac{8}{9}(\tilde{b}^2 + \bar{w}) > \tilde{m}^2$, the only critical point is the minimum at $\tilde{r}_0 = 0$.

Let us come back to the zeros of $Q^{\bar{w}}_{\tilde{b}}$. Regarded a function of the complex variable $\tilde{r} \in \mathbb{C}$, it has 4 zeros on the complex plane; only those on the positive real axis are physically relevant though. Furthermore, regarded a function on the full real line, $Q^{\bar{w}}_{\tilde{b}}(\tilde{r})$ is the sum of 4 terms all of which are positive if $\tilde{r} < 0$. As a consequence, $Q^{\bar{w}}_{\tilde{b}}$ has no zeros at strictly negative $\tilde{r}$. *A priori* $Q^{\bar{w}}_{\tilde{b}}$ could have 4 zeros at $\tilde{r} > 0$. This case is already excluded, however, since we saw that the function has at most one maximum and one minimum at strictly positive $\tilde{r}$. Therefore, as far as zeros at $\tilde{r} > 0$ are concerned, only the following 3 cases can occur: (a) 2 simple zeros, (b) 1 double zero, and (c) no zero at all.

In Fig. 3 we show an example of each case. In this figure and all similar diagrams the notation $\tilde{r}^I_{\tilde{b}_\pm}$ stands for either $\tilde{r}^I_{H_\pm} \equiv \tilde{r}^I_\pm$ or $\tilde{r}^I_{S_\pm}$, depending on the interpretation of $\tilde{b}$.

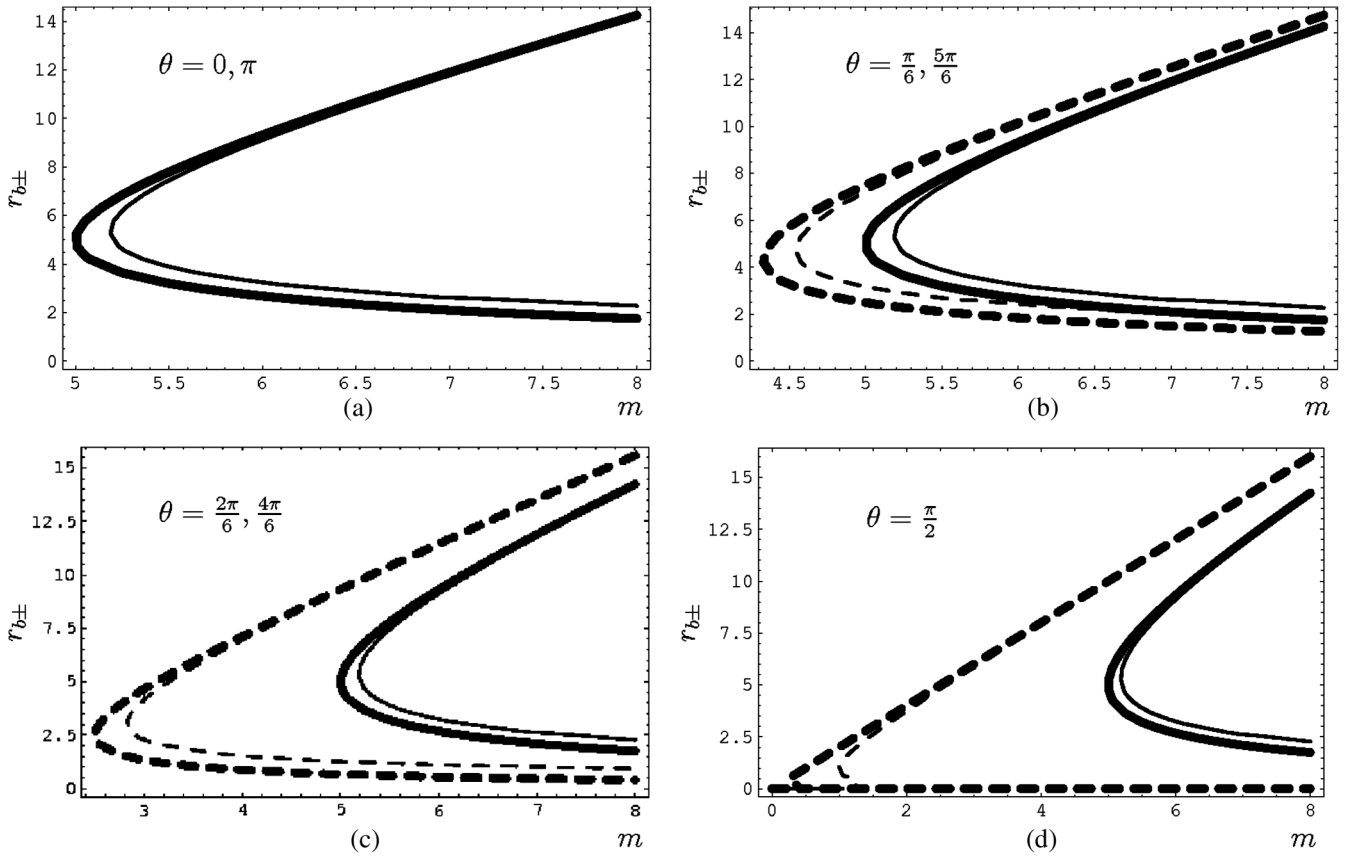

FIG. 4. The figures show the m dependence of the radii $r_{b\pm}$ (thick lines) and $r^I_{b\pm}$ (thin lines) for $a = 5$ and several values of θ. The continuous lines represent $r_\pm$ and $r^I_\pm$. The dashed lines represent $r_{S\pm}$ and $r^I_{S\pm}$.

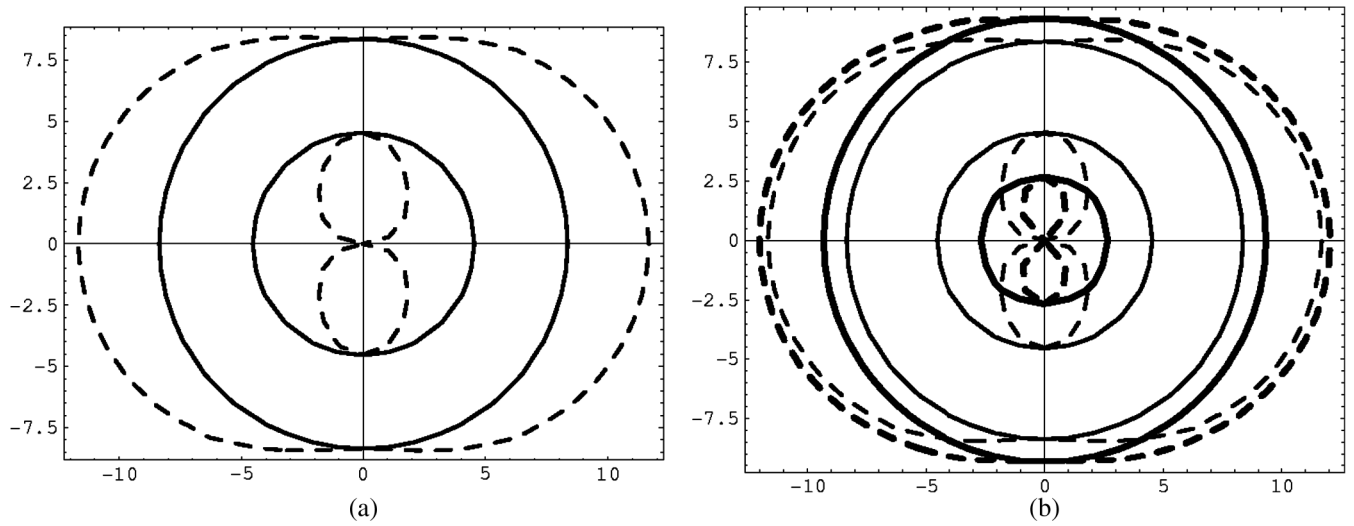

FIG. 5. The figures show a cross section through the event horizons (continuous lines) and static limit surfaces (dashed lines) in the xz plane for a quantum black hole with $\tilde{m} = 6$ and $\tilde{a} = 5$. To facilitate the comparison with the classical case, in (b) the corresponding classical surfaces are superimposed (thick lines).

The superscript "I" indicates that the respective radii refer to the improved metric.

From the definition of $Q^{\bar{w}}_{\tilde{b}}$, Eq. (4.6), it is obvious that the occurrence of zeros is the more likely the larger is $\tilde{m}$ and the smaller are $\tilde{b}$ and $\bar{w}$. The reason is that for $\tilde{m}$ large and $\tilde{b}$ and $\bar{w}$ small the second term on the RHS of (4.6), $-2\tilde{m}\tilde{r}^3 < 0$, becomes very negative and the positive terms $(\tilde{b}^2 + \bar{w})\tilde{r}^2 > 0$ and $\bar{w}\tilde{b}^2 > 0$ are small which favors zeros. Therefore we expect that, for $\tilde{a}$ (and $\bar{w}$) fixed, there are two zeros for large $\tilde{m}$ [case (a)] and no zero for small $\tilde{m}$ [case (c)]. In between there is a critical mass at which the extremal situation of a simple double zero is realized [case (b)].

In Fig. 4 we show that this is indeed the case. Here the radii of both horizons and critical limit surfaces are displayed; this amounts to $\tilde{b} = \tilde{a}$ and $\tilde{b} = \tilde{a}\cos\theta$ in the formulas above. In all diagrams we fixed $\tilde{a} = 5$ (and $\bar{w} = 1$) and plotted the classical and improved radii as a function of $\tilde{m}$. The 4 diagrams correspond to different values of θ. Generically [cases (b) and (c)] we find 4 different improved radii $\tilde{r}^I_{\pm}$, $\tilde{r}^I_{S_\pm}(\theta)$ when $\tilde{m}$ is very large. When we lower $\tilde{m}$ we reach a point at which the two horizons coalesce, $\tilde{r}^I_+ = \tilde{r}^I_-$, and below which there is no horizon any longer, but there still exist two critical limit surfaces. Lowering $\tilde{m}$ even further the two static limit surfaces coalesce at a certain critical mass, $\tilde{r}^I_{S_+}(\theta) = \tilde{r}^I_{S_-}(\theta)$, and for even smaller $\tilde{m}$ there exists neither a horizon nor a static limit surface.

Figure 4(a) applies to the poles ($\theta = 0, \pi$) where the event horizons and static limit surfaces touch, $\tilde{r}^I_+ = \tilde{r}^I_{S_+}(\theta)$, $\tilde{r}^I_- = \tilde{r}^I_{S_-}(\theta)$. Figure 4(d) refers to the equatorial plane ($\theta = \pi/2$) in which, classically, $r_{S_-} = 0$, $r_{S_+} = 2m$.

In the two-dimensional diagrams of Fig. 5 we display the θ dependence of the various radii. Here we picked the parameter values $\tilde{m} = 6$, $\tilde{a} = 5$ for which there exist two horizons $H_\pm$ and two static limits $S_\pm$. (For the constant $\bar{w}$ we chose $\bar{w} = 4$.)

Both Figs. 4 and 5 show that the quantum effects are the larger the smaller is $\tilde{m}$. For $\tilde{m} \equiv M/m_{\rm Pl} \gg 1$ the critical surfaces of the improved black hole coincide essentially with those of the classical one. Lowering M we find that the radius of the outer horizon H_+ is always smaller than in the classical case, while the radius of H_- is always larger than classically. Similarly we see that $\tilde{r}^I_{S_+}(\theta) < \tilde{r}_{S_+}(\theta)$ whereas $\tilde{r}^I_{S_-}(\theta) > \tilde{r}_{S_-}(\theta)$. Both for horizons and static limits the extremal points where the upper and the lower branches of the curves meet are shifted towards larger masses by the quantum corrections.

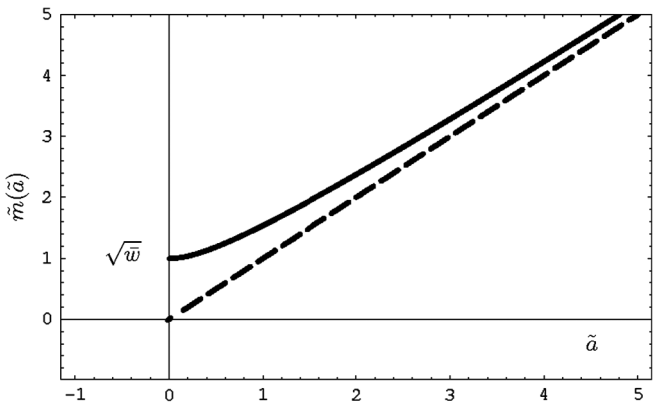

FIG. 6. The solution $\tilde{m}(\tilde{a})$ of the quantum extremality condition for the improved Kerr black hole [with $d(r) = r$ and $\bar{w} = 1$]. The dashed line represents the $\tilde{m}(\tilde{a}) = \tilde{a}$ dependence of the classical Kerr spacetime. For $\tilde{a} \to 0$, $\tilde{m}$ assumes its minimum value at $\sqrt{\bar{w}}$, while it approaches the classical behavior for $\tilde{a} \to \infty$.

C. The quantum extremality condition

Let us determine the condition on $\tilde{m}$ and $\tilde{b}$ which implies a double zero of $Q^{\bar{w}}_{\tilde{b}}(\tilde{r})$. If $b = a$, this is the condition for the two horizons H_+ and H_- to coincide, i.e. for the quantum black hole to be extremal. When $Q^{\bar{w}}_{\tilde{b}}(\tilde{r})$ has a double zero at some value of $\tilde{r}$, the function must have a (local) minimum there. Since $\tilde{r} = \tilde{r}_2$ of (4.17) is the only minimum it has for $\tilde{r} > 0$, it follows that the extremal case is realized precisely if $Q^{\bar{w}}_{\tilde{b}}$ vanishes at $\tilde{r}_2$: $Q^{\bar{w}}_{\tilde{b}}(\tilde{r}_2)|_{\text{extremal}} = 0$. Inserting (4.17) into (4.6) we obtain

$$Q^{\bar{w}}_{\tilde{b}}(\tilde{r}_2) = -\frac{27\tilde{m}^4}{32}\left[\left(1 - \frac{8}{9}\frac{\tilde{b}^2 + \bar{w}}{\tilde{m}^2}\right)^{(3/2)} + \frac{8}{27}\frac{(\tilde{b}^2 - \bar{w})^2}{\tilde{m}^4} - \frac{4}{3}\frac{\tilde{b}^2 + \bar{w}}{\tilde{m}^2} + 1\right]. \tag{4.19}$$

As a result, setting $b = a$, the condition for $H_+ = H_-$ reads

$$\left(1 - \frac{8}{9}\frac{\tilde{a}^2 + \bar{w}}{\tilde{m}^2}\right)^{(3/2)} + \frac{8}{27}\frac{(\tilde{a}^2 - \bar{w})^2}{\tilde{m}^4} - \frac{4}{3}\frac{\tilde{a}^2 + \bar{w}}{\tilde{m}^2} + 1 = 0. \tag{4.20}$$

We shall refer to (4.20) as the "quantum extremality condition." If $\bar{w} = 0$, it reduces to $\tilde{m} = \tilde{a}$ for the classical Kerr metric, and if $\tilde{a} = 0$, to $\tilde{m} = \sqrt{\bar{w}}$, which is the correct result for the extremal version of the improved Schwarzschild black hole; see Ref. [28]. In the general case $\bar{w} \neq 0$, $\tilde{a} \neq 0$ the condition (4.20) can be solved for $\tilde{m} = \tilde{m}(\tilde{a})$ only numerically. The result is shown in Fig. 6. We observe that $\tilde{m}(\tilde{a})$ approaches the classical $\tilde{m} = \tilde{a}$ for large a but deviates significantly for $\tilde{a} \to 0$.

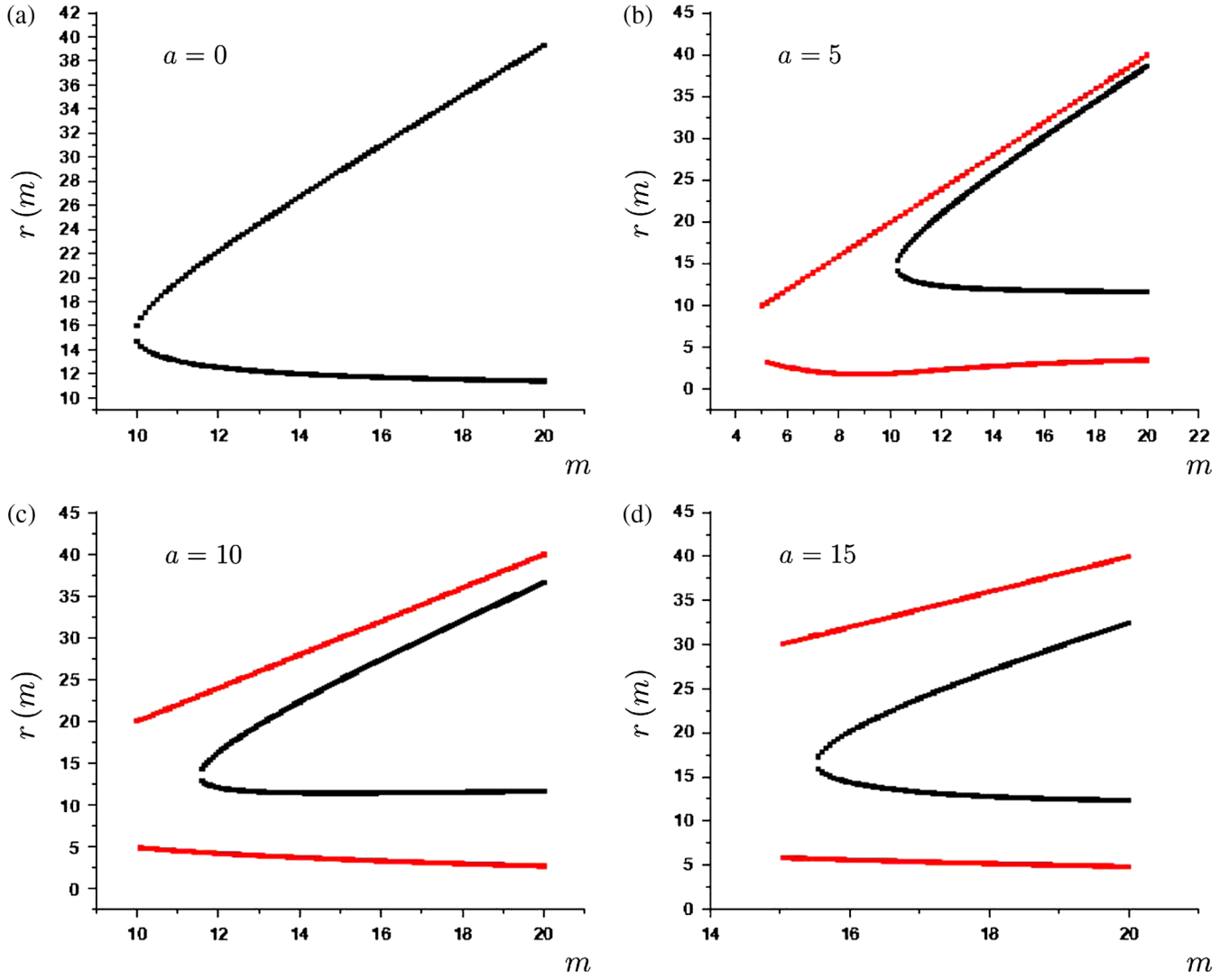

FIG. 7 (color online). The figures show the m dependence of the improved radii $r^I_{b\pm}$ obtained from the exact $d(r)$ given in (2.5) at $\theta = \frac{\pi}{2}$, for $\bar{w} = 5$ and several values of a. The outer curves are the improved static limits $r^I_{S\pm}$ and the inner ones the improved event horizons $r^I_{\pm}$. The structure of the curves is essentially the same as in the $d(r) = r$ approximation.

D. Exact distance function

Up to now we employed the simplified distance function $d(r) = r$, which has the virtue that all calculations can be performed analytically. Using numerical techniques we have repeated the above analysis for the "exact" distance function (2.5) and (2.6). It turns out that, qualitatively, the results found with the exact $d(r)$ are exactly the same as those from the $d(r) = r$ approximation. This concerns, in particular, the number of horizons and critical surfaces, the systematics of their mass and angular momentum dependence, and their disappearing at extremal configurations. (See Fig. 7 for an example.)

Thus one of the main results is that the classical and the improved Kerr metrics, sufficiently far away from extremality, have *the same* number of horizons and static limit surfaces. This was different for the Schwarzschild metric: The classical spacetime has 1 horizon, but the improved spacetime has 2. So, *a priori* one might have expected a similar doubling in the case of the Kerr metric. Actually this is not what happens: The quantum corrections do not generate new critical surfaces but rather smoothly deform the classical ones.

In the language of "catastrophe theory" [54,55] this can be understood from the structural stability properties of the zeros and critical points of $Q_{\tilde{b}}^{\bar{w}}$. The corresponding function for the classical Schwarzschild metric has a "structurally unstable" triple zero at $\tilde{r} = 0$; giving a nonzero value to $\bar{w}$ it dissolves into a double zero at $\tilde{r} = 0$ and a simple one at $\tilde{r} > 0$. The very same transition from a triple to a double plus a simple zero happens to the Kerr metric already classically by a nonzero value of $\tilde{a}$. If, in addition, the quantum parameter $\bar{w} \propto O(\hbar)$ is given a nonzero value, no further zero is generated. It is easy to formally prove the structural stability of the classical Kerr zeros [49].

V. PENROSE PROCESS

One of the most remarkable features of rotating black holes is the possibility of extracting energy from them, by means of the Penrose process, for instance [45]. This is possible since under certain kinematical conditions test particles in the Kerr metric can be in a state of negative energy. In fact, let us consider a composite system A, consisting of two particles B and C, which crosses the static limit. It disintegrates into B and C near the event horizon whereby particle B is in a state of negative energy. Subsequently B falls through the horizon, thus making a negative contribution to the black hole's internal energy. The other particle, C, leaves the ergosphere and reaches its final state at infinity. The conservation of the total energy for the black hole and the test particles implies an increased energy for the test particle C. The energy it gains equals minus the change in the internal energy of the black hole.

As the possibility of energy extraction is intimately limited to the existence of negative energy states we shall now analyze this issue for the improved Kerr metric in order to get a first impression of the impact the quantum gravity corrections have on the region of the test particle phase space with $E < 0$.

The conserved energy of a point particle is given by Eq. (3.9). If we use BL coordinates and parametrize its trajectory by the proper time τ, we have explicitly, with the angular velocity $\Omega \equiv d\varphi/dt$,

$$E = -mt^{\mu} g_{\mu\nu} \frac{dx^{\nu}}{d\tau} = -m\left[g_{tt} \frac{dt}{d\tau} + g_{\varphi t} \frac{d\varphi}{d\tau} \right] = -m\left[g_{tt} + g_{\varphi t}\Omega \right] \frac{dt}{d\tau}. \tag{5.1}$$

Using the explicit form of the improved Kerr metric the negative energy constraint $E \leq 0$ boils down to

$$\Omega \leq \Omega_0 \equiv -\frac{g_{tt}}{g_{\varphi t}} = \frac{2MG(r)r - \rho^2}{2MG(r)ra\sin^2\theta}. \tag{5.2}$$

Following [45] it is convenient to reexpress the inequality (5.2) in terms of the tangential "bookkeeper velocity"

$$v_{\tan} \equiv R(r,\theta)\frac{d\varphi}{dt} = R(r,\theta)\Omega \tag{5.3}$$

with the reduced circumference

$$R(r,\theta) \equiv \sqrt{g_{\varphi\varphi}} = \sqrt{\frac{\Sigma_I \sin^2\theta}{\rho^2}}. \tag{5.4}$$

(The reduced circumference is defined such that $ds^2 = R^2 d\varphi^2$ if $dt = dr = d\theta = 0$.) In terms of $v_{\tan}$ the negative energy condition $\Omega \leq \Omega_0$ becomes $v_{\tan} \leq R\Omega_0$, or

$$v_{\tan}(r) \leq v_0 \equiv R(r,\theta)\left(\frac{2MG(r)r - \rho^2}{2MG(r)ra\sin^2\theta}\right). \tag{5.5}$$

In the following we shall restrict our analysis to the equatorial plane, $\theta = \pi/2$. In this case the condition (5.5) assumes the form

$$v_{\tan}(r) \leq \frac{1}{a}\sqrt{r^2 + a^2 + \frac{2Ma^2G(r)}{r}}\left(1 - \frac{r}{2MG(r)}\right) = v_0^{\mathrm{eq}}(r). \tag{5.6}$$

Here v_0^{eq} denotes the bookkeeper tangential velocity, i.e. the velocity referring to the *coordinate* time t of a particle which moves in the equatorial plane and has vanishing energy $E = 0$.

The phase space for the rotational motion of a massive test particle is bounded by the $v(r)$ curves for co- and counterrotating light rays:

$$v_{-}^{\mathrm{light}}(r) < v_{\tan}(r) < v_{+}^{\mathrm{light}}(r). \tag{5.7}$$

The bookkeeper tangential velocities for light follow from (3.15):

$$v_{\pm}^{\mathrm{light}}(r) = R(r,\theta)\Omega_{\pm} = R(r,\theta)\left(\omega \pm \sqrt{\omega^2 - \frac{g_{tt}}{g_{\varphi\varphi}}}\right). \tag{5.8}$$

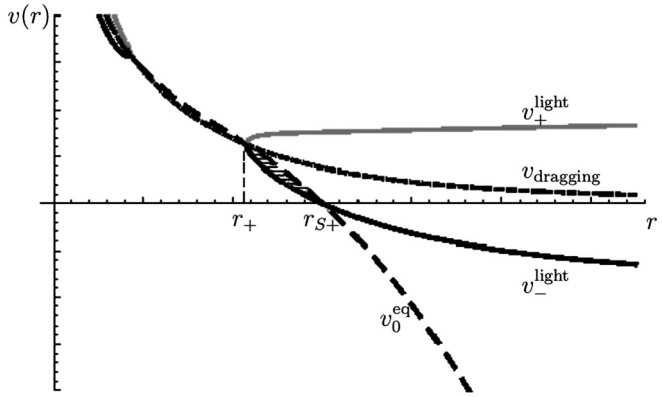

FIG. 8. The figure shows schematically the r dependence of $v_{\pm}^{\text{light}}$, v_0^{eq}, and v_{dragging} at the equatorial plane. The hatched region corresponds to pairs (r, v) for which the test particle has negative energy.

In the (r, v_{tan}) plane, the part of the test particle phase space corresponding to $E < 0$ is obtained by intersecting the regions defined by the inequalities (5.6) and (5.7), respectively.

The situation is sketched qualitatively in Fig. 8. Besides $v_{\pm}^{\text{light}}$ and v_0^{eq} the figure shows also the r dependence of the dragging velocity $v_{\text{dragging}} = R(r, \theta)\omega$. It is not difficult to prove that for any function $G(r)$, the v_0^{eq} and v_{-}^{light} curves intersect at the static limit $(r = r_{S_+})$ and that $v_0^{\text{eq}} = v_{+}^{\text{light}} = v_{-}^{\text{light}} = v_{\text{dragging}}$ at the horizon $(r = r_+)$.

In Figs. 9 and 10 we show the corresponding realistic plots which were obtained numerically. Figure 9 corresponds to the classical and Fig. 10 to the improved case. All plots refer to the equator, $\theta = \pi/2$, and in the improved case the function $G(r)$ was taken as in Eq. (4.3) with $d(r) = r$. Next to each (r, v) plot we display the M dependence of the radii $r_{\pm}$ and $r_{S\pm}$ and indicate by a dashed vertical bar the M value used in the corresponding plot on the LHS. This presentation makes it obvious if, and how many, critical surfaces exist for the corresponding M value.

When varying the mass $m = MG$ in Figs. 9 and 10 we keep the ratio a/m fixed. The reason is that, classically, $r_{\pm}$ and $r_{S\pm}$ are *linear* functions of m if we readjust a such that $a/m = \text{const}$; see Eqs. (1.9) and (1.10). As a consequence, the negative energy region for the classical metric changes

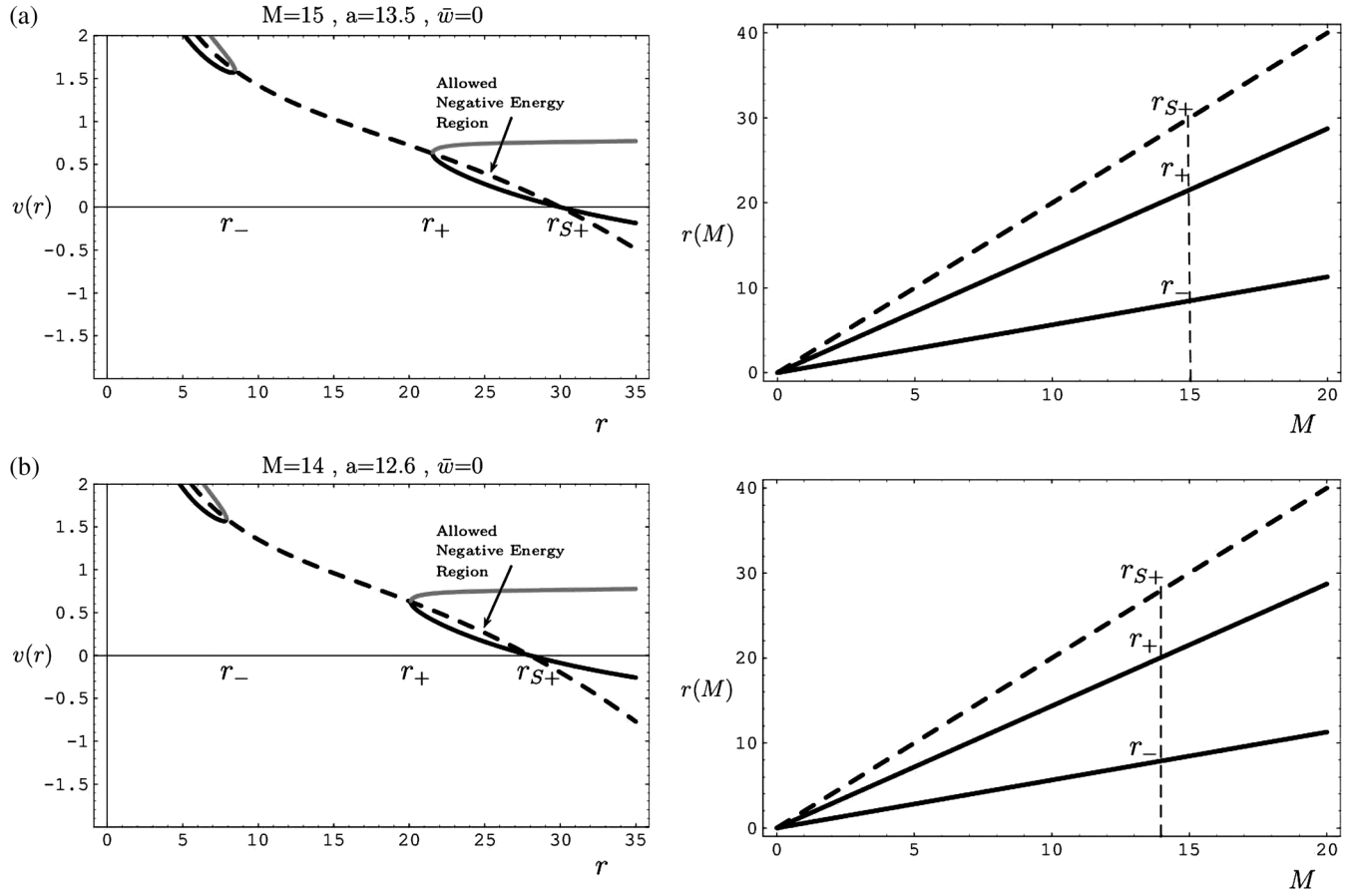

FIG. 9. The plots on the LHS of this figure display the r dependence of $v_{\pm}^{\text{light}}$ and v_0^{eq} and are analogous to Fig. 8. They refer to classical Kerr black holes with $M = 15m_{\text{pl}}$, $a = 13.5m_{\text{pl}}$ and $M = 15m_{\text{pl}}$, $a = 12.6m_{\text{pl}}$, respectively. They have the same ratio $a/m = 0.9$. On the RHS the radius of the critical surfaces is displayed for all masses up to $20m_{\text{pl}}$, for the constant ratio $a/m = 0.9$ as in the corresponding plots on the LHS. The dashed vertical line in the plots on the RHS symbolizes the mass values used on the LHS.

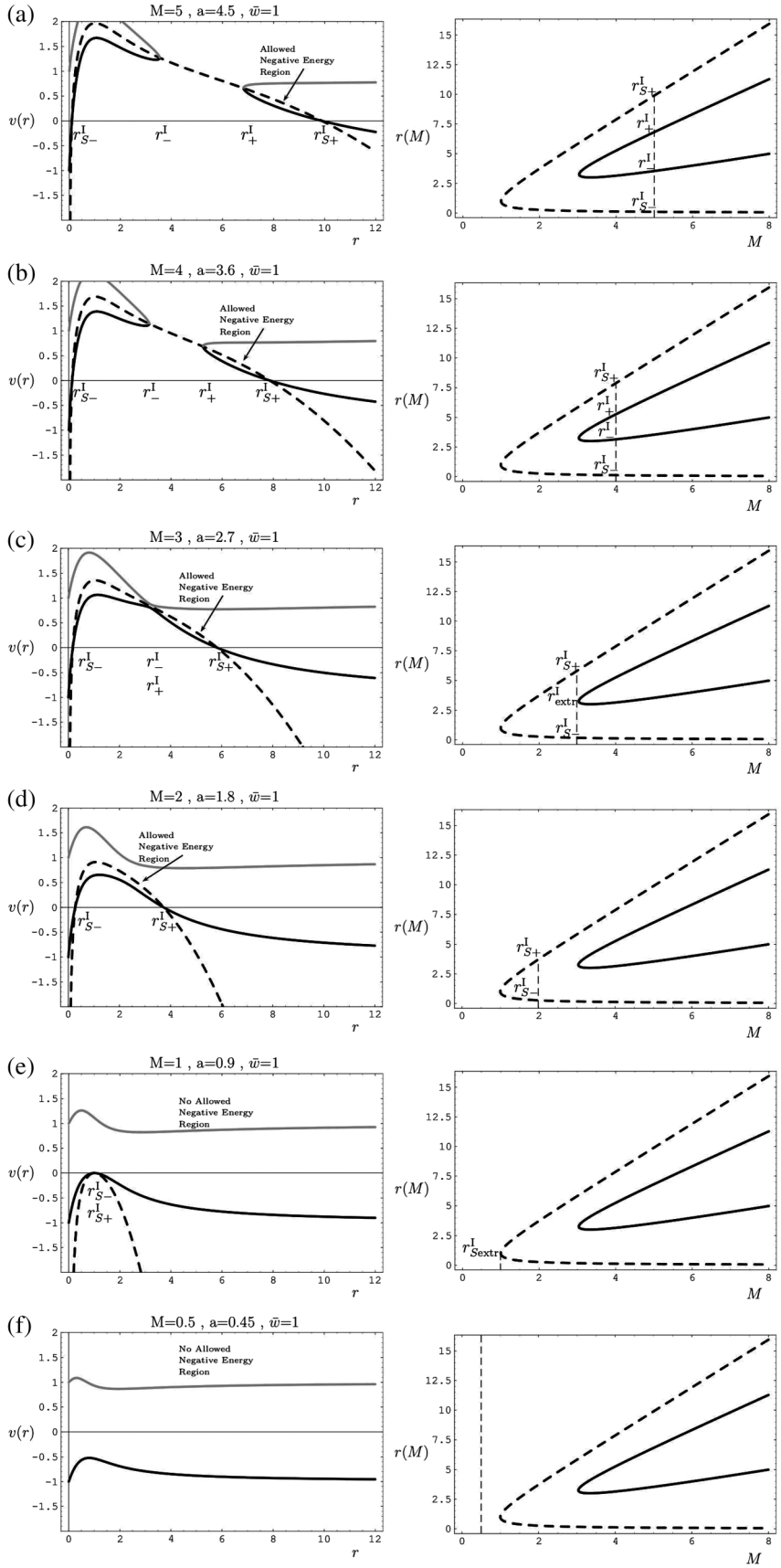

FIG. 10. The same type of plots as in Fig. 9, but now for the improved Kerr black hole, with masses ranging from $M = 5m_{\rm pl}$ down to $M = 0.5m_{\rm pl}$. All examples considered have an identical ratio $a/m = 0.9$.

its size with m but not its shape. This can be seen in Fig. 9. Hence changes of the shape are entirely due to the quantum effects.

Figure 10(a) shows the region of negative energy for $M = 5m_{\rm pl}$, $a = 4.5$. Since we are still sufficiently away from the Planck region the shape of the improved negative energy region is not too different from the classical one. In Fig. 10(b) we have changed M from 5 to 4 Planck masses for which the shape of the negative energy region is almost unchanged. Besides the $E < 0$ region discussed above, Figs. 10(a) and 10(b) show an internal negative energy region bounded by $r^I_{S_-}$ and r^I_-. Since the possibility of extraction of energy relies on the existence of stationary states with negative energy outside r^I_+, the internal region cannot be considered physically relevant.

Figures 10(c)–10(f) were obtained for the regime $M \approx m_{\rm pl}$. Drastic changes in the shape of the negative energy regions are visible. Since the reliability of our method is questionable in this regime, conclusions about this region have to be considered with some care. We analyze these cases nevertheless since they hint at the possibility of interesting new features.

In Fig. 10(c) the quantum extremal black hole with $M = M_{\rm cr}$ and $r^I_- = r^I_+ = r^I_{\rm extr}$ has been reached. The internal and external negative energy regions touch at $r^I_{\rm extr}$.

Figure 10(d) shows a hypothetical configuration for $M < M_{\rm cr}$ with two static limits $S^I_\pm$ and no event horizon. The internal and external negative energy regions merged into just one. This region is bounded by the static limit surfaces at $r^I_{S_-}$ and $r^I_{S_+}$. In this case there exists an ergosphere from where energy can be extracted, but no horizons.

Figures 10(e) and 10(f) show configurations in which no extraction of energy is possible. At the extremal static limit configuration shown in Fig. 10(e) the negative energy region is reduced to zero size.

This analysis suggests that, while it is possible to extract energy from classical black holes with arbitrarily small masses and angular momenta, there exists a lowest mass for the Penrose mechanism in the improved Kerr spacetime. It is close to the Planck mass and defined by the extremal static limit. However, since the reliability of our method is questionable in the regime $M \approx m_{\rm pl}$, it would be desirable to investigate this possibility by independent methods.

VI. VACUUM ENERGY-MOMENTUM TENSOR AND ENERGY CONDITIONS

We may reinterpret the RG-improved vacuum Kerr metric $g^{\rm imp}_{\mu\nu}$ as a *classical* spacetime in the presence of matter. Knowing $g^{\rm imp}_{\mu\nu}$ explicitly, we can compute its Einstein tensor and insist on the validity of the classical field equation

$$G_{\mu\nu}(g^{\rm imp}) = 8\pi G_0 T^Q_{\mu\nu}. \tag{6.1}$$

This equation then defines a vacuum energy-momentum tensor which describes the energy and momentum of a fictitious "pseudomatter" which reproduces the quantum corrections found by the RG improvement by means of the conventional Einstein equation. The explicit calculation yields, after a fair amount of algebra,

$$T^Q_{\mu\nu}(r,\theta) = \frac{M}{32\pi G_0\rho^6\Delta}\begin{bmatrix} q_1 & 0 & 0 & \upsilon \\ 0 & q_2 & 0 & 0 \\ 0 & 0 & q_3 & 0 \\ \upsilon & 0 & 0 & q_4 \end{bmatrix} \tag{6.2}$$

with the entries ($n = 1, 2, 3, 4$)

$$\begin{aligned} q_n(r,\theta) &\equiv \alpha_n(r,\theta)G'(r) + \beta_n(r,\theta)G''(r), \\ \upsilon(r,\theta) &\equiv \alpha_\nu(r,\theta)G'(r) + \beta_\nu(r,\theta)G''(r). \end{aligned} \tag{6.3}$$

Here the coefficient functions are given by

$$\begin{aligned} \alpha_1(r,\theta) \equiv& -(a^2+r^2)[8r^2(a^2+r^2) - a^4(\sin 2\theta)^2] \\ & - 16ra^2MG\sin^2\theta\cos^2\theta, \end{aligned} \tag{6.4}$$

$$\alpha_2 \equiv 8r^2\Delta^2, \qquad \alpha_3 \equiv 8\Delta a^2\cos^2\theta, \tag{6.5}$$

$$\begin{aligned} \alpha_4 &\equiv \csc^2\theta\alpha_3 - 8a^2r^2, \\ \alpha_\nu &\equiv 8ar^2(r^2+a^2) - a\alpha_3, \end{aligned} \tag{6.6}$$

$$\beta_1(r,\theta) \equiv 4\Delta r\rho^2a^2\sin^2\theta, \qquad \beta_2(r,\theta) \equiv 0, \tag{6.7}$$

$$\beta_3(r,\theta) \equiv 4\Delta r\rho^2, \qquad \beta_4(r,\theta) \equiv 4\Delta r\rho^2\csc^2\theta, \tag{6.8}$$

$$\beta_\nu(r,\theta) \equiv -4a\Delta r\rho^2. \tag{6.9}$$

The rows and columns of the $T^Q_{\mu\nu}$ matrix above are ordered in the sequence $t - r - \theta - \varphi$. The matrix is diagonal except for the $t\varphi$ entry. A nonzero value of $T^Q_{t\varphi}$ was to be expected, of course, since this corresponds precisely to matter rotating about the z axis.

It is not difficult to diagonalize $T^Q_{\mu\nu}$. In its eigenbasis it reads

$$T^Q_{\mu\nu}(r,\theta) = \frac{M}{32\pi G_0\rho^6\Delta}\,{\rm diag}[l_1, l_2, l_3, l_4] \tag{6.10}$$

with the diagonal matrix elements

$$\begin{aligned} l_1 &\equiv \tfrac{1}{2}[q_1 + q_4 + \sqrt{q_1^2 - 2q_1q_4 + q_4^2 + 4\upsilon^2}], \\ l_2 &\equiv q_2, \\ l_3 &\equiv q_3, \\ l_4 &\equiv \tfrac{1}{2}[q_1 + q_4 - \sqrt{q_1^2 - 2q_1q_4 + q_4^2 + 4\upsilon^2}]. \end{aligned} \tag{6.11}$$

Despite the formal analogy it would be premature to conclude that the vacuum quantum effects can be mimicked by the presence of matter. The reason is that $T^Q_{\mu\nu}$ turns out to violate all the positivity conditions which are

usually assumed to be satisfied by physically realizable matter [56]. For a diagonalized energy-momentum tensor $T^{\nu}_{\mu} = \mathrm{diag}[-\rho, p_1, p_2, p_3]$ one distinguishes the following "energy conditions" [48,56]:

$$\begin{aligned}&\text{weak energy condition: } \rho \geq 0,\ \rho + p_i > 0;\\ &\text{null energy condition: } \rho + p_i \geq 0;\\ &\text{dominant energy condition: } \rho \geq 0,\ \rho \geq |p_i|;\\ &\text{strong energy condition: } \rho + p_i \geq 0,\ \rho + \sum_i p_i \geq 0.\end{aligned} \tag{6.12}$$

From (6.10) with (6.11) we can read off the energy density ρ and the pressures p_i, $i = 1, 2, 3$, corresponding the energy-momentum tensor $T^{Q}_{\mu\nu}$. It is then straightforward to check numerically whether or not the energy conditions (6.12) are satisfied. The result is that *all four energy conditions are violated, at least in a part of the improved Kerr spacetime.*

This result does not come completely unexpected; also the vacuum expectation value of energy-momentum operators (as in the case of the Casimir effect, for instance) typically violates the energy conditions. As a consequence, the quantum gravity effects are qualitatively different from those due to ordinary matter. From the practical point of view this means that the analysis of the improved black hole does not reduce to applying the many known results and theorems which are available for classical black holes with matter. The reason is that in most cases their derivation assumes the validity of one or the other of the conditions (6.12). For instance, for deriving the focusing theorem for timelike geodesic congruences from Raychaudhuri's equation one needs the strong energy condition [48]. Furthermore, the thermodynamics of the improved black holes is *not* a special case of the familiar (semi)classical black-hole thermodynamics with matter.

VII. DRESSING OF MASS AND ANGULAR MOMENTUM

The improved Kerr metric describes an isolated object in an asymptotically flat spacetime. As this spacetime possesses the two Killing vectors $\boldsymbol{t}$ and $\boldsymbol{\varphi}$ we can ascribe a mass and an angular momentum to this object by means of the Komar integrals [48,57]:

$$M_{\mathrm{Komar}} = -\frac{1}{8\pi G_0}\int_S \nabla^{\alpha} t^{\beta} dS_{\alpha\beta}, \tag{7.1}$$

$$J_{\mathrm{Komar}} = \frac{1}{16\pi G_0}\int_S \nabla^{\alpha} \varphi^{\beta} dS_{\alpha\beta}. \tag{7.2}$$

Here S is a two-sphere at spatial infinity. Its surface element $dS_{\alpha\beta}$ is given by $dS_{\alpha\beta} = -2n_{[\alpha}r_{\beta]}\sqrt{\sigma}d^2\theta$, where n_{α} and r_{α} are the timelike and spacelike normals to S, respectively. Here σ is the determinant of σ_{ab}, the metric induced from $g_{\alpha\beta}$ in the 2D surface S, and $d^2\theta \equiv d\theta^1 d\theta^2$ with θ^a angular coordinates on S. The integrals for M_{Komar} and J_{Komar} probe the metric only at spatial infinity. Since the improved Kerr metric equals the classical one far away from the black hole, the values of M_{Komar} and J_{Komar} are not changed by the RG improvement. It is well known [48] that for the classical Kerr metric they coincide with the mass and angular momentum parameters which it contains:

$$M_{\mathrm{Komar}} = M, \qquad J_{\mathrm{Komar}} = J. \tag{7.3}$$

Thus, for S a surface at spatial infinity, (7.3) holds true also in the improved case.

The mass and angular momentum of the object as measured at infinity receive a contribution from the pseudomatter mimicking the quantum effects. To identify it we break up M_{Komar} and J_{Komar} into two pieces, one which contains only the effect of the pseudomatter within the outer horizon $H \equiv H_+$ and one which is due to the matter distribution outside H. The first contribution yields quantities M_H and J_H, which we refer to as the mass and angular momentum of the black hole, respectively, meaning here only the portion of space bounded by H. The second contribution describes the "dressing" of this intrinsic mass and angular momentum by matter external to the black hole.

The relation between the parameters M and J calculated at the spatial infinity and the quantities M_H and J_H calculated at the event horizon can be derived if we consider a 3D spacelike hypersurface Σ extending from the event horizon to spatial infinity. Its inner boundary is H, a two-dimensional cross section of the event horizon, and its outer boundary is S. Using Gauss' theorem and the field equation (6.1) we find that M and J can be decomposed as

$$M = M_H + 2\int_{\Sigma}\left(T^{Q}_{\alpha\beta} - \frac{1}{2}T^{Q}g_{\alpha\beta}\right)n^{\alpha}t^{\beta}\sqrt{h}d^3y, \tag{7.4}$$

$$J = J_H - \int_{\Sigma}\left(T^{Q}_{\alpha\beta} - \frac{1}{2}T^{Q}g_{\alpha\beta}\right)n^{\alpha}\varphi^{\beta}\sqrt{h}d^3y. \tag{7.5}$$

Here h_{ab} is the metric induced in Σ, and y^a ($a = 1, 2, 3$) are coordinates intrinsic to this hypersurface. M_H and J_H are the "genuine" black-hole mass and angular momentum, respectively. They are given by surface integrals over H:

$$M_H = -\frac{1}{8\pi G_0}\int_H \nabla^{\alpha} t^{\beta} ds_{\alpha\beta}, \tag{7.6}$$

$$J_H = \frac{1}{16\pi G_0}\int_H \nabla^{\alpha} \varphi^{\beta} ds_{\alpha\beta}. \tag{7.7}$$

The surface element $ds_{\alpha\beta} = 2\xi_{[\alpha}N_{\beta]}\sqrt{\sigma}d^2\theta = (\xi_{\alpha}N_{\beta} - \xi_{\beta}N_{\alpha})\sqrt{\sigma}d^2\theta$ involves an auxiliary null vector N_{α} which satisfies $N_{\alpha}\xi^{\alpha} = -1$ and $N_{\alpha}N^{\alpha} = 0$ [48].

The relations (7.4) and (7.5) can be interpreted as follows: The total mass M (angular momentum J) is given by a contribution M_H (J_H) from the black hole, plus a contribution from the matter distribution outside. If the black

hole is in vacuum, then $M = M_H$ and $J = J_H$. According to the discussion of Sec. VI we expect that $M_H \neq M$ and $J_H \neq J$ when the contributions of the "quantum fluid" are taken into account, i.e. that the mass and the angular momentum of the black hole get "renormalized" or dressed by the matter surrounding it. This interpretation is confirmed by an explicit evaluation of the integrals (7.6) and (7.7). The calculation is somewhat lengthy but similar to the classical one. The final answer reads [49]

$$M_H = M\frac{G(r_+)}{G_0}\left\{1 - \left[\frac{(r_+^2 + a^2)G'(r_+)}{aG(r_+)}\right]\arctan\left(\frac{a}{r_+}\right)\right\}, \quad (7.8)$$

$$J_H = \left\{J + \left[1 - \frac{2MG(r_+)}{a}\arctan\left(\frac{a}{r_+}\right)\right]\left[\frac{M^2G'(r_+)r_+^2}{a}\right]\right\} \times \frac{G(r_+)}{G_0}. \quad (7.9)$$

These results have a number of remarkable properties:

(A) One can verify that for any pair of black-hole parameters, (M, J), the ratio M_H/M is always *smaller* than unity; it approaches unity only asymptotically, for $M \to \infty$, when the quantum effects become insignificant. The interpretation is that the black hole possesses a genuine (positive) mass M_H to which the quantum matter adds another *positive* contribution to make up the mass measured at infinity, M. Given the fact that the pseudomatter satisfies no standard positivity condition it is by no means trivial that M is larger than M_H. However this is exactly what one would expect if quantum gravity is *antiscreening*: The metric fluctuations dress any test mass (here the black-hole interior) in such a way that the mass increases with the distance [1]. The same is found to hold true for the angular momentum: J_H/J is always smaller than unity; i.e. the pseudomatter increases the spin of the test mass.

(B) Despite their somewhat complicated structure, the results (7.8) and (7.9) satisfy the same Smarr formula which is valid for classical black holes [49,58]:

$$M_H = 2\Omega_H J_H + \frac{\kappa\mathcal{A}}{4\pi G_0}. \quad (7.10)$$

Here Ω_H and κ are given by the improved equations (3.21) and (3.31), respectively, and $\mathcal{A}$ denotes the surface of the outer horizon H. Both in the classical and the improved case it can be written as

$$\mathcal{A} = 4\pi(r_+^2 + a^2), \quad (7.11)$$

but for improved black holes the dependence of r_+ on M and J (or a) is much more complicated.

(C) The results (7.8) and (7.9) are strikingly similar to the corresponding formulas for the *classical* Kerr-Newman spacetime [48] which, besides mass and angular momentum, is characterized by an electric charge Q. The expressions coincide *exactly* if we identify

$$Q^2 \triangleq 2Mr_+^2G'(r_+)/G_0. \quad (7.12)$$

This coincidence does not come completely unexpected. In [27] where the $a = 0$ case had been analyzed, it turned out that the improved Schwarzschild metric has many features in common with the classical Reissner-Nordström metric [a minimum of the lapse function $f(r)$, causal structure, etc.]. For $a \neq 0$ there is still a corresponding similarity between the improved Kerr metric and the classical Kerr-Newman spacetime. The exact coincidence of the Komar integrals is somewhat surprising though. It is intriguing to speculate that it might have a deeper meaning.

VIII. A MODIFIED FIRST LAW OF BLACK-HOLE THERMODYNAMICS

The first law of *classical* black-hole thermodynamics states that the 1-form $2\pi(\delta M - \Omega_H\delta J)/\kappa$ is exact, i.e. that it can be written as the differential of a state function $S = S(M, J)$. Hence

$$\delta M - \Omega_H\delta J = T\delta S, \quad (8.1)$$

where one interprets

$$T(M, J) = \frac{\kappa(M, J)}{2\pi} \quad (8.2)$$

and S as the black-hole temperature and entropy, respectively [51,59]. In terms of its surface area $\mathcal{A}$ the latter is given by $S = \mathcal{A}/4G_0$ [60]. For these results to hold the functions (zero forms) κ and Ω_H must have a very special M and J dependence. In Sec. III we found the corresponding relations for the improved case, namely,

$$\kappa(M, J) = \frac{r_+^I - M[r_+^IG'(r_+^I) + G(r_+^I)]}{(r_+^I)^2 + (J/M)^2}, \quad (8.3)$$

$$\Omega_H(M, J) = \frac{(J/M)}{(r_+^I)^2 + (J/M)^2}. \quad (8.4)$$

Here $r_+^I \equiv r_+^I(M, J)$, but this relationship cannot be written down in closed form.

In this section we analyze whether the RG-improved black holes satisfy a quantum-corrected version of the first law (8.1) and, if so, how the temperature and entropy get modified.

A. Preliminaries

The states an improved Kerr black hole can be in are labeled by the two parameters M and J. We visualize the corresponding state space as (part of) the two-dimensional

Euclidean plane with Cartesian coordinates $x^1 = M$, $x^2 = J$. Using the convenient language of differential forms, state functions are zero forms on this space, i.e. scalars $f = f(x) \equiv f(M, J)$. Defining the exterior derivative as[1]

$$\delta = \delta M \frac{\partial}{\partial M} + \delta J \frac{\partial}{\partial J}$$

a differential form $\boldsymbol{\alpha}$ is *closed* if $\delta\boldsymbol{\alpha} = 0$, and it is *exact* if $\boldsymbol{\alpha} = \delta\boldsymbol{\beta}$, where $\boldsymbol{\beta}$ denotes a $(p-1)$-form when $\boldsymbol{\alpha}$ is a p-form. The state space being two-dimensional, the only case of interest is $p = 1$. A general 1-form has the expansion $\boldsymbol{\alpha} = P(M, J)\delta M + N(M, J)\delta J$. This 1-form is closed if

$$\frac{\partial P}{\partial J} = \frac{\partial N}{\partial M} \tag{8.5}$$

and it is exact if there exists a 0-form $S(M, J)$ such that $\boldsymbol{\alpha} = \delta S$ or, in components, $P = \partial S/\partial M$, $N = \partial S/\partial J$. We assume that the states (M, J) form a simply connected subset of the Euclidean plane so that $\delta\boldsymbol{\alpha} = 0$ is necessary and sufficient for the exactness of $\boldsymbol{\alpha}$.

If $\boldsymbol{\alpha}$ is not exact, one can try to find an integrating factor $\mu(M, J)$ such that the product $\mu\boldsymbol{\alpha}$ is exact: $\mu(M, J)\boldsymbol{\alpha} = \delta S$. Hence $\delta(\mu\boldsymbol{\alpha}) = 0$, or $\partial(\mu P)/\partial J = \partial(\mu N)/\partial M$, which implies a quasilinear partial differential equation for the 0-form $\mu(M, J)$ [61–63]:

$$P\left(\frac{\partial \mu}{\partial J}\right) - N\left(\frac{\partial \mu}{\partial M}\right) = \mu\left[\left(\frac{\partial N}{\partial M}\right) - \left(\frac{\partial P}{\partial J}\right)\right]. \tag{8.6}$$

B. Does there exist an entropylike state function?

The 1-form we are actually interested in is

$$\boldsymbol{\alpha} = \frac{2\pi}{\kappa(M, J)}(\delta M - \Omega_H(M, J)\delta J) \tag{8.7}$$

with

$$P \equiv \frac{2\pi}{\kappa}, \qquad N \equiv -\frac{2\pi\Omega_H}{\kappa} \tag{8.8}$$

involving the surface gravity and angular velocity of Eqs. (8.3) and (8.4). The crucial question is whether $\boldsymbol{\alpha}$ is closed, i.e. whether its components (8.8) satisfy the integrability condition (8.5). The explicit calculation reveals that for a generic $G(r)$ this is actually *not* the case: The 1-form (8.7) with the quantum-corrected versions of κ and Ω_H is not closed and, as a consequence, not exact. [This calculation is straightforward, in principle, but rather tedious [49]. One has to be careful about differentiating all the implicit M and J dependencies that enter via $r_+^I(M, J)$. One does not need the explicit form of this function; its partial derivatives can be expressed in terms of r_+^I itself by differentiating the horizon condition $\Delta(r_+^I) = 0$.]

[1]To conform with the standard notation of thermodynamics we denote the exterior derivative by δ rather than d.

As $\boldsymbol{\alpha}$ is not exact in the improved case we must conclude that there does *not* exist a differential relation of the type

$$\delta M - \Omega_H \delta J = \left(\frac{\kappa}{2\pi}\right)\delta\left(\frac{\mathcal{A}}{4G_0} + \text{quantum corrections}\right) \tag{8.9}$$

which could play the role of a modified first law for quantum black holes. The interpretation of (8.9) would have been clear: The Bekenstein-Hawking temperature of the improved black holes is related to the surface gravity by $T = \kappa/2\pi$, as in the classical case, and there exists a state function $S(M, J)$ which equals the classical $\mathcal{A}/4G_0$ plus correction terms. Since $\boldsymbol{\alpha}$ is actually not exact we must conclude that *either there exists no entropylike state function for the improved black holes or the classical relation $T = \kappa/2\pi$ does not hold true for them.*

We see that for quantum Kerr black holes even the very existence of an entropy is a nontrivial issue. The situation was different for the improved Schwarzschild black holes [28]. Since there the state space is one-dimensional, $\boldsymbol{\alpha} \equiv (2\pi/\kappa)\delta M$ is trivially exact, $T = \kappa/2\pi$ continues to be valid, and the entropy one finds has indeed the structure $\mathcal{A}/4G_0$ + quantum corrections [28,29].

Thus we are led to conclude that if there exists a modified, i.e. quantum, version of black-hole thermodynamics which is accessible by RG improvement, then the temperature cannot be simply proportional to the surface gravity: $T \neq \kappa/2\pi$. While *a priori* it is perhaps not very surprising that the semiclassical relation $T = \kappa/2\pi$ is subject to quantum gravity correction, this causes a difficulty of principle. Within the present approach we were able to find the corrected M and J dependence of κ and Ω_H, and, as a result, we know the corrected 1-form $\boldsymbol{\alpha}$. However, without additional input, knowledge of $\boldsymbol{\alpha}$ is not enough to deduce the two functions $T(M, J)$ and $S(M, J)$. There exist infinitely many pairs (T, S) such that $\boldsymbol{\alpha} = T\delta S$ for a prescribed $\boldsymbol{\alpha}$. In a full-fledged quantum gravity version of black-hole thermodynamics it might be possible to find the ''correct'' one, presumably.

A general theory of this kind is beyond the scope of the present paper. Here we only consider the possible structure of a modified first law. As we shall see in the next subsection, progress can be made by restricting the discussion to black holes of small angular momentum. To leading order in a J^2 expansion the corrections to the temperature and entropy are found to be uniquely fixed.

C. Temperature and entropy to order J^2

By time reflection symmetry, the small-J expansions of the temperature and entropy read

$$T(M, J) = T_0(M) + T_2(M)J^2 + O(J^4), \tag{8.10}$$

$$S(M,J) = S_0(M) + S_2(M)J^2 + O(J^4). \tag{8.11}$$

The terms of lowest order, $T_0(M)$ and $S_0(M)$, refer to the RG-improved Schwarzschild spacetime [28,29]. They satisfy $\delta M = T_0 \delta S_0$ or $1/T_0(M) = dS_0(M)/dM$. In [28] this relation has been integrated in order to find the entropy of the improved Schwarzschild black hole:

$$S_0 = \int_{M_{\rm cr}}^{M} \frac{dM'}{T_0(M')}. \tag{8.12}$$

In the approximation $d(r) = r$ the temperature was found to be given by

$$\begin{aligned} T_0(M) &= \frac{1}{4\pi G_0 M_{\rm cr}} \frac{\sqrt{Y(1-Y)}}{1+\sqrt{1-Y}} \\ &= \frac{1}{8\pi G_0 M}\left[1 - \frac{1}{4}\left(\frac{M_{\rm cr}}{M}\right)^2 - \frac{1}{8}\left(\frac{M_{\rm cr}}{M}\right)^4 + O(M^{-6})\right]. \end{aligned} \tag{8.13}$$

Here $Y \equiv M_{\rm cr}^2/M^2$ and $M_{\rm cr} \equiv \sqrt{\bar{w}} m_{\rm Pl}$. (The critical mass $M_{\rm cr}$ is the smallest mass for which the improved Schwarzschild spacetime has an event horizon [28].) Using (8.13) in (8.12) yields

$$\begin{aligned} S_0(M) &= S_0(M_{\rm cr}) + 2\pi\bar{w}[Y^{-1}\sqrt{1-Y}(1+\sqrt{1-Y}) \\ &\quad + \arctan\sqrt{1-Y}] \\ &= S_0(M_{\rm cr}) + \frac{\mathcal{A}^{\rm Sch}_{\rm Class}}{4G_0} + 2\pi\bar{w}\left[\ln\left(\frac{2M}{M_{\rm cr}}\right) - \frac{3}{2}\right. \\ &\quad \left. - \frac{3}{8}\left(\frac{M_{\rm cr}}{M}\right)^2 - \frac{5}{32}\left(\frac{M_{\rm cr}}{M}\right)^4 + O(M^{-6})\right]. \end{aligned} \tag{8.14}$$

Here $\mathcal{A}^{\rm Sch}_{\rm Class} \equiv 4\pi(2G_0M)^2$ is the classical Schwarzschild surface area. The first few terms of the large-M expansions given in (8.13) and (8.14) are rather reliable predictions probably since for $M \gg m_{\rm Pl}$ the classical spacetime is only weakly distorted by quantum effects.

Next we try to determine T_2 and S_2 such that $\delta M - \Omega_H \delta J = T\delta S$ is satisfied to order J^2. Inserting the *Ansätze* for T and S we have

$$\begin{aligned} \delta M - \Omega_H \delta J &= [T_0(M) + T_2(M)J^2]\delta[S_0(M) + S_2(M)J^2] \\ &= T_0\delta S_0 + \delta S_0 T_2 J^2 + \delta(S_2 J^2)T_0 + O(J^3). \end{aligned} \tag{8.15}$$

Exploiting that $T_0\delta S_0 = \delta M$ we are left with

$$\begin{aligned} -\Omega_H \delta J &= \delta S_0 T_2 J^2 + \delta(S_2 J^2)T_0 + O(J^3) \\ &= T_2 J^2\left(\frac{dS_0}{dM}\right)\delta M + T_0\left[J^2\left(\frac{dS_2}{dM}\right)\delta M + 2JS_2\delta J\right] \\ &\quad + O(J^3). \end{aligned} \tag{8.16}$$

Equating the coefficients of δJ and δM we find the following two coupled equations which determine S_2 and T_2:

$$T_2\left(\frac{dS_0}{dM}\right) + T_0\left(\frac{dS_2}{dM}\right) = 0 + O(J^4), \tag{8.17}$$

$$2JT_0S_2 + \Omega_H = 0 + O(J^3). \tag{8.18}$$

In Eq. (8.18) we need Ω_H to linear order in J only. From (8.4) we obtain

$$\Omega_H(M,J) = \frac{J}{M r^I_{\rm Sch+}(M)^2} + O(J^3), \tag{8.19}$$

where $r^I_{\rm Sch+} \equiv r^I_+(J=0)$ refers to the improved Schwarzschild black hole. In the approximation $d(r) = r$ we are using here this radius is explicitly given by [28]

$$r^I_{\rm Sch+} = G_0 M[1 + \sqrt{1-Y}]. \tag{8.20}$$

With (8.19) in (8.18) we can solve for the function S_2:

$$S_2(M) = -[2MT_0(M)r^I_{\rm Sch+}(M)^2]^{-1}. \tag{8.21}$$

Furthermore, taking advantage of $dS_0/dM = 1/T_0$ again, we can solve (8.17) for T_2 in terms of the, by now known, function S_2:

$$T_2(M) = -T_0(M)^2 \frac{dS_2(M)}{dM}. \tag{8.22}$$

In deriving the relations (8.21) and (8.22) we were able to find a well defined and *unique* answer for the coefficients of the J^2 terms. Equation (8.21) for $S_2(M)$ involves only the known Schwarzschild quantities T_0 and $r^I_{\rm Sch+}$, and once S_2 is known also T_2 is completely fixed by Eq. (8.22).

Using the results from the Schwarzschild case we obtain the following final result for the temperature and entropy to order J^2:

$$\begin{aligned} T(M,J) &= \frac{1}{8\pi G_0 M}\left[1 - \frac{1}{4}\left(\frac{M_{\rm cr}}{M}\right)^2 - \frac{1}{8}\left(\frac{M_{\rm cr}}{M}\right)^4 + O(M^{-6})\right] \\ &\quad - \frac{J^2}{32\pi M^5 G_0^3}\left[1 + \left(\frac{M_{\rm cr}}{M}\right)^2 + \frac{15}{16}\left(\frac{M_{\rm cr}}{M}\right)^4\right. \\ &\quad \left. + O(M^{-6})\right] + O(J^4), \end{aligned} \tag{8.23}$$

$$\begin{aligned} S(M,J) &= \frac{\mathcal{A}^{\rm Sch}_{\rm class}}{4G_0} + 2\pi\bar{w}\left[\ln\left(\frac{2M_{\rm cr}}{M}\right) - \frac{3}{2} - \frac{3}{8}\left(\frac{M_{\rm cr}}{M}\right)^2\right. \\ &\quad \left. - \frac{5}{32}\left(\frac{M_{\rm cr}}{M}\right)^4 + O(M^{-6})\right] - \left(\frac{\pi J^2}{M^2 G_0}\right) \\ &\quad \times\left[1 + \frac{3}{4}\left(\frac{M_{\rm cr}}{M}\right)^2 + \frac{5}{8}\left(\frac{M_{\rm cr}}{M}\right)^4 + O(M^{-6})\right] \\ &\quad + O(J^4). \end{aligned} \tag{8.24}$$

In writing down the result for the entropy we fixed the undetermined constant of integration such that $S = 0$ for $M = M_{\rm cr}$ and $J = 0$.

We observe that the angular momentum-dependent terms in (8.23) and (8.24) *decrease* both the black hole's temperature and entropy as compared to the corresponding Schwarzschild quantities. We also see that the size of the J^2 corrections increases with $M_{\rm cr}/M$; i.e. these corrections grow as the mass M of the black hole becomes smaller during the evaporation process.

In summarizing the most important aspects of the modified black-hole thermodynamics discussed in this section we recall that $2\pi T$ does not agree with the surface gravity κ here as it is the case in the familiar (semi)classical situation. We demonstrated that a modified first law can exist only when we give up the relationship $T = \kappa/2\pi$. We also showed that, to order J^2, there is a uniquely determined modification of this relationship which allows for the existence of a state function $S(M, J)$ with the interpretation of an entropy.

IX. SUMMARY AND CONCLUSION

In this paper we tried to assess the impact of the leading quantum gravity corrections on the properties of rotating black holes within the framework of quantum Einstein gravity. Using the gravitational average action as the basic tool we developed a scale-dependent picture of the spacetime structure. We exploited that Γ_k is a family of effective field theories labeled by k. More precisely, to each point $\mathcal{P}$ we associated a coarse-graining scale $k = k(\mathcal{P})$ and then described a neighborhood of $\mathcal{P}$ by the specific effective action $\Gamma_{k(\mathcal{P})}$. In principle, there could be several plausible choices of the map $\mathcal{P} \to k(\mathcal{P})$. They lead to different ''pictures'' of the same physical system. Using the analogy of a microscope with a variable resolving power [25] we are using a microscope with a position-dependent resolving power, and clearly the picture we see depends on how we change the resolving power from point to point. For the black hole the choice of $k(\mathcal{P})$ is made less ambiguous than for a generic spacetime since we would like the picture, the improved metric, to have the same symmetries as the classical metric. We chose $k(\mathcal{P})$ to be monotonically decreasing in the radial direction, giving the best ''resolution'' to points near the black hole and the worst to those asymptotically far away. The experience with similar RG improvements indicates that in this way the improved metric encodes the leading quantum corrections at least at a qualitative level.

The results we obtained can be summarized as follows. In general, the quantum corrections are small for heavy black holes ($M \gg m_{\rm Pl}$) but become appreciable for light ones. Heavy quantum black holes have the same number of critical surfaces as the classical ones, namely, two static limit surfaces and two horizons. (For $J = 0$ the improvement had led to the formation of a new horizon.) As one lowers M towards the Planck mass, the two horizons coalesce and then disappear. At an even smaller mass the static limit surfaces coalesce and then disappear as well.

Even though the reliability of the improvement method becomes questionable when the corrected metric is very different from the classical one we believe that the disappearance of the horizons below a certain critical mass is a fairly reliable prediction. In fact, this phenomenon has a very simple interpretation: The existence of a horizon means that the gravitational field is so strong that it can trap light; if, however, the strength of the gravitational interaction is reduced at small distances by the RG running of G, then it is quite plausible that very small objects with a low mass cannot prevent light from escaping.

Whether or not these objects have a naked singularity remains an open question. The method used here is likely to lose its validity close to the black hole's center. Also on the basis of earlier investigations [28], it is likely though that the quantum corrections soften the singularity (again because G is switched off at short distances); it is even conceivable that it disappears altogether [28].

A particularly intriguing feature of the Kerr black hole is the possibility of energy extraction. As the Penrose process is related to the existence of negative energy states of test particles we analyzed the phase space of such negative energy states in detail. In particular, we saw that, while it is possible to extract energy from classical black holes of arbitrary small mass and angular momentum, in the improved Kerr spacetime there exists a minimum mass for energy extraction. It is defined by the extremal configuration of the static limit surfaces.

We explained that even though the quantum black holes in the vacuum can be reinterpreted as classical black holes in the presence of a special kind of matter mimicking the quantum fluctuations, many of their mechanical and, in particular, thermodynamical properties are nevertheless nonstandard since this pseudomatter does not satisfy any of the familiar energy conditions.

As a first step towards an ''RG-improved black-hole thermodynamics'' we analyzed the problem of identifying a state function which could possibly be interpreted as an entropy. We saw that in the quantum case the 1-form $(\delta M - \Omega_H \delta J)/\kappa$ is no longer exact or, stated differently, the surface gravity is not an integrating factor of $\delta M - \Omega_H \delta J$. We concluded that if an entropy is to exist also for the improved black hole, their temperature cannot simply be proportional to κ. We also saw that for small angular momentum, to order J^2, there exist unambiguously defined modified relationships for the M and J dependence of temperature and entropy. We hope to come back to a more detailed discussion of these thermodynamical issues elsewhere.

ACKNOWLEDGMENTS

E. T. thanks the German Service of Academic Exchange (DAAD) and the Institute of Physics in Mainz for the financial support during the development of his Ph.D. thesis.

[1] M. Reuter, Phys. Rev. D **57**, 971 (1998).

[2] S. Weinberg, in *General Relativity, An Einstein Centenary Survey*, edited by S. W. Hawking and W. Israel (Cambridge University Press, Cambridge, England, 1979); arXiv:hep-th/9702027; arXiv:0903.0568; Proc. Sci., CD09 (2009) 001 [arXiv:0908.1964]; arXiv:0911.3165.

[3] D. Dou and R. Percacci, Classical Quantum Gravity **15**, 3449 (1998).

[4] O. Lauscher and M. Reuter, Phys. Rev. D **65**, 025013 (2001).

[5] M. Reuter and F. Saueressig, Phys. Rev. D **65**, 065016 (2002).

[6] O. Lauscher and M. Reuter, Phys. Rev. D **66**, 025026 (2002).

[7] O. Lauscher and M. Reuter, Classical Quantum Gravity **19**, 483 (2002).

[8] O. Lauscher and M. Reuter, Int. J. Mod. Phys. A **17**, 993 (2002).

[9] W. Souma, Prog. Theor. Phys. **102**, 181 (1999).

[10] M. Reuter and F. Saueressig, Phys. Rev. D **66**, 125001 (2002); Fortschr. Phys. **52**, 650 (2004).

[11] A. Bonanno and M. Reuter, J. High Energy Phys. 02 (2005) 035.

[12] For reviews see O. Lauscher and M. Reuter, in *Quantum Gravity*, edited by B. Fauser, J. Tolksdorf, and E. Zeidler (Birkhäuser, Basel, 2007); in *Approaches to Fundamental Physics*, edited by I.-O. Stamatescu and E. Seiler (Springer, Berlin, 2007); M. Reuter and F. Saueressig, arXiv:0708.1317.

[13] R. Percacci and D. Perini, Phys. Rev. D **67**, 081503 (2003); **68**, 044018 (2003); Classical Quantum Gravity **21**, 5035 (2004).

[14] A. Codello and R. Percacci, Phys. Rev. Lett. **97**, 221301 (2006); A. Codello, R. Percacci, and C. Rahmede, Int. J. Mod. Phys. A **23**, 143 (2008).

[15] D. Litim, Phys. Rev. Lett. **92**, 201301 (2004); P. Fischer and D. Litim, Phys. Lett. B **638**, 497 (2006).

[16] P. Machado and F. Saueressig, Phys. Rev. D **77**, 124045 (2008).

[17] O. Lauscher and M. Reuter, J. High Energy Phys. 10 (2005) 050.

[18] M. Reuter and J.-M. Schwindt, J. High Energy Phys. 01 (2006) 070.

[19] M. Reuter and J.-M. Schwindt, J. High Energy Phys. 01 (2007) 049.

[20] M. Reuter and H. Weyer, Phys. Rev. D **79**, 105005 (2009).

[21] P. Forgács and M. Niedermaier, arXiv:hep-th/0207028; M. Niedermaier, J. High Energy Phys. 12 (2002) 066; Nucl. Phys. **B673**, 131 (2003); Classical Quantum Gravity **24**, R171 (2007).

[22] For detailed reviews of asymptotic safety in gravity see M. Niedermaier and M. Reuter, Living Rev. Relativity **9**, 5 (2006), http://relativity.livingreviews.org/Articles/lrr-2006-5; R. Percacci, arXiv:0709.3851.

[23] C. Wetterich, Phys. Lett. B **301**, 90 (1993).

[24] M. Reuter and C. Wetterich, Nucl. Phys. **B417**, 181 (1994); **B427**, 291 (1994); **B391**, 147 (1993); **B408**, 91 (1993); M. Reuter, Phys. Rev. D **53**, 4430 (1996); Mod. Phys. Lett. A **12**, 2777 (1997).

[25] J. Berges, N. Tetradis, and C. Wetterich, Phys. Rep. **363**, 223 (2002); C. Wetterich, Int. J. Mod. Phys. A **16**, 1951 (2001).

[26] For reviews of the effective average action in Yang-Mills theory see M. Reuter, arXiv:hep-th/9602012; J. Pawlowski, Ann. Phys. (N.Y.) **322**, 2831 (2007); H. Gies, arXiv:hep-ph/0611146.

[27] A. Bonanno and M. Reuter, Phys. Rev. D **60**, 084011 (1999).

[28] A. Bonanno and M. Reuter, Phys. Rev. D **62**, 043008 (2000).

[29] A. Bonanno and M. Reuter, Phys. Rev. D **73**, 083005 (2006).

[30] M. Reuter and E. Tuiran, arXiv:hep-th/0612037.

[31] A. Bonanno and M. Reuter, Phys. Rev. D **65**, 043508 (2002); M. Reuter and F. Saueressig, J. Cosmol. Astropart. Phys. 09 (2005) 012.

[32] A. Bonanno and M. Reuter, Phys. Lett. B **527**, 9 (2002); Int. J. Mod. Phys. D **13**, 107 (2004); E. Bentivegna, A. Bonanno, and M. Reuter, J. Cosmol. Astropart. Phys. 01 (2004) 001.

[33] A. Bonanno and M. Reuter, J. Cosmol. Astropart. Phys. 08 (2007) 024.

[34] A. Bonanno, G. Esposito, and C. Rubano, Gen. Relativ. Gravit. **35**, 1899 (2003); Classical Quantum Gravity **21**, 5005 (2004); A. Bonanno, G. Esposito, C. Rubano, and P. Scudellaro, Classical Quantum Gravity **23**, 3103 (2006); **24**, 1443 (2007).

[35] M. Reuter and H. Weyer, Phys. Rev. D **69**, 104022 (2004).

[36] M. Reuter and H. Weyer, Phys. Rev. D **70**, 124028 (2004).

[37] M. Reuter and H. Weyer, J. Cosmol. Astropart. Phys. 12 (2004) 001.

[38] K. Falls, D. Litim, and A. Raghuraman, arXiv:1002.0260; Y. Cai and D. A. Easson, J. Cosmol. Astropart. Phys. 09 (2010) 002.

[39] A. Satz, F. D. Mazzitelli, and E. Alvarez, Phys. Rev. D **71**, 064001 (2005); A. Satz, A. Codello, and F. D. Mazzitelli, Phys. Rev. D **82**, 084011 (2010).

[40] Robert H. Boyer and Richard W. Lindquist, J. Math. Phys. (N.Y.) **8**, 265 (1967).

[41] R. P. Kerr, Phys. Rev. Lett. **11**, 237 (1963).

[42] J. Cohen, J. Math. Phys. (N.Y.) **9**, 905 (1968).

[43] B. Carter, Phys. Rev. Lett. **26**, 331 (1971).

[44] R. Adler, M. Bazin, and M. Schiffer, *Introduction to General Relativity* (McGraw-Hill, New York, 1965).

[45] Edwin F. Taylor and John A. Wheeler, *Exploring Black Holes, Introduction to General Relativity* (Addison-Wesley, Reading, MA, 2000).

[46] D. Christodolou, Phys. Rev. Lett. **25**, 1596 (1970); Ph.D. thesis, Princeton University, 1971 (unpublished); D. Christodolou and R. Ruffini, Phys. Rev. D **4**, 3552 (1971).

[47] Charles W. Misner, Kip S. Thorne, and John A. Wheeler, *Gravitation* (Freeman, San Francisco, 1973).

[48] E. Poisson, *A Relativist's Toolkit* (Cambridge University Press, Cambridge, England, 2004).

[49] E. Tuiran, Ph.D. thesis, Mainz University, 2007.

[50] J. Lense and H. Thirring, Phys. Z. **19**, 156 (1918).

[51] J. M. Bardeen, B. Carter, and S. W. Hawking, Commun. Math. Phys. **31**, 161 (1973).

[52] I. Ràcz and R. Wald, Classical Quantum Gravity **13**, 539 (1996).

[53] J. M. Bardeen, Nature (London) **226**, 64 (1970).

[54] T. Poston and I. Stewart, *Catastrophe Theory and Its Applications* (Dover, New York, 1978).
[55] J. Milnor, *Morse Theory* (Princeton University, Princeton, NJ, 1963).
[56] S. W. Hawking and G. F. R. Ellis, *The Large Scale Structure of Space-Time* (Cambridge University Press, Cambridge, England, 1973).
[57] A. Komar, Phys. Rev. **113**, 934 (1959).
[58] L. Smarr, Phys. Rev. Lett. **30**, 71 (1973).
[59] J. D. Bekenstein, Lett. Nuovo Cimento **4**, 737 (1972); Phys. Rev. D **7**, 2333 (1973).
[60] S. W. Hawking, Phys. Rev. Lett. **26**, 1344 (1971).
[61] G. Simmons, *Differential Equations with Applications and Historical Notes* (McGraw-Hill, New York, 1972).
[62] R. Courant and D. Hilbert, *Methods of Mathematical Physics* (Wiley, New York, 1962), Vol. II.
[63] C. Caratheodory, *Variationsrechnung* (Teubner, Berlin, 1935).